AN ABSTRACT OF THE THESIS OF

Pitak Chuawong for the degree of Master of Science in Chemistry presented on August 6, 2001. Title: Synthesis, Characterization, and Reactivity of Rhenium Dithiodiolate and Monothiodiolate Complexes.

Redacted for Privacy

Abstract Approved: _____
Kevin P. Gable

The rhenium dithiodiolate, Hydrido-*tris*-(3,5-dimethyl-1-pyrazolyl) borato(ethane-1,2-dithiodiolato)(oxo)rhenium(V), and Hydrido-*tris*-(3,5-dimethyl-1-pyrazolyl)borato(phenylethanedithiodiolato)(oxo)rhenium(V), were synthesized by reductive cyclocondensation of alkane-1,2-dithiols with Tp'ReO_3 in a one pot fashion. The rhemium monothiodiolate, Hydrido-*tris*-(3,5-dimethyl-1-pyrazolyl) borato(ethane-1,2-monothiodiolato)(oxo)rhenium(V), and Hydrido-*tris*-(3,5-dimethyl-1-pyrazolyl)borato(propanemonothiodiolato)(oxo)rhenium(V), were also synthesized by using the same procedure. The *syn* and *anti* isomers of rhenium phenylethanedithiodiolate and rhenium propanemonothiodiolate were characterized by using COSY, nOe, and HSQC experiments. An X-ray crystal structure of the rhenium ethanedithiodiolate was obtained, and an unusually small dihedral angle (S-C-C-S) of about 12^{o} was observed. The solution conformation of these compounds was investigated by using a Karplus relationship between vicinal

coupling constants and dihedral angle. The dihedral angle for the ethanedithiodiolate appeared to be 38° indicating a staggered geometry for the ring.

All of these complexes failed to cyclorevert to any detectable extent at 120°C after 7 days. This observation reflects the thermal stability of rhenium dithiodiolate and monothiodiolate complexes. Energetics of ethylene addition to tetrathioperrhenate anion (ReS_4^-) and addition of hydrogen sulfide to the alkene adduct were calculated by DFT calculation using LACVP** basis set with B3LYP functionals. The heat of reaction of ethylene addition to ReS_4^- was –15.4 kcal/mol, and –111.1 kcal/mol for addition of hydrogen sulfide to the alkene adduct. These results are consistent with the stability of the dithiodiolate complex toward cycloreversion reaction.

Reaction of Tp'ReO_3 and ethylene sulfide led to the rhenium ethanedithiolate complex both with and without acid catalysis. This observation led to a proposed multi step mechanism.

Synthesis, Characterization, and Reactivity of Rhenium Dithiodiolate and Monothiodiolate Complexes

By

Pitak Chuawong

A THESIS

submitted to

Oregon State University

in partial fulfillment of
the requirements for the
degree of

Master of Science

Presented August 6, 2001
Commencement June 2002

Master of Science thesis of Pitak Chuawong presented on August 6, 2001

APPROVED:

Redacted for Privacy

Major Professor, representing Chemistry

Redacted for Privacy

Chair of Department of Chemistry

Redacted for Privacy

Dean of Graduate School

I understand that my thesis will become part of the permanent collection of Oregon State University libraries. My signature below authorizes release of my thesis to any reader upon request.

Redacted for Privacy

Pitak Chuawong, Author

ACKNOWLEDGEMENTS

I would like to express my gratitude to my research advisor, Dr. Gable, who helped me in every step of my research and gave me valuable suggestions for my thesis writing. His support and encouragement are highly appreciated. I would also like to thank Dr. Alex Yokochi for obtaining crystal structure of Hydridotris(3,5-dimethyl-1-pyrazolyl)borato(ethane-1,2-dithiodiolato)(oxo)rhenium(V). Help from Dr. Gable's group, Eric Brown, Fedor Zhuravlev, and Scott Allen is also appreciated. I am grateful to the DPST program of the Royal Thai Government for financial support. Finally, I would like to thank my family for being very supportive in my graduate study.

TABLE OF CONTENTS

Page

Chapter 1. Introduction and Literature Review.....1

1.1. Formation of C-O and C-S Bond By Transition Metal Complexes.....1

1.2. Dihydroxylation of Olefins by OsO_4 and Mechanistic Study.....5

1.3. Use of Rhenium Diolates for Study of Dihydroxylation Reaction of Olefins.....7

1.4. Cycloreversion of Cp* Rhenium (V) Diolates.....8

1.5. Cycloreversion of Tp' Rhenium (V) Diolates.....10

1.6. Report of Alkenes Extrusion from Cp* Rhenium (V) Dithiodiolate.....11

1.7. Binding of Alkene to Tetrathioperrhenate Anion (ReS_4^-) and Influence of Hydrogensulfide and Thiols.....13

1.8. Sturctures and Synthesis of Tp Rhenium Ethanedithiodiolate Complex...15

1.9. Catalytic Deoxygenation of Epoxides Using Tp' Rhenium Oxide.....18

1.10. Reaction of Ethylene Sulfide and Propylene Sulfide with $Cp'ReCl_4$.....20

1.11. Conclusions of the Literature Review.....22

Chapter 2. Results and Discussion.....23

2.1. Cycloreversion of Rhenium Diolates.....23

2.2. Synthesis and Characterization of Hydrido-*tris*-(3,5-dimethyl-1-pyrazolyl)borato(ethane-1,2-dithiodiolato)(oxo)rhenium(V) 25

2.3. Synthesis and Characterization of Hydrido-*tris*-(3,5-dimethyl-1-pyrazolyl)borato(ethane-1,2-monothiodiolato)(oxo)rhenium(V) 28

2.4. Synthesis and Characterization of Hydrido-*tris*-(3,5-dimethyl-1-pyrazolyl)borato(propanemonothiodiolato)(oxo)rhenium(V) 29

TABLE OF CONTENTS (Continued)

Page

2.5. nOe Experiment with *Anti*-Isomer of Tp' Rhenium Propanemonothiodiolate.....30

2.6. nOe Experiment with *Syn*-Isomer of Tp' Rhenium Propanemonothiodiolate.....32

2.7. Synthesis of Phenylethane-1,2-dithiol 34

2.8. Synthesis and Characterization of Hydrido-*tris*-(3,5-dimethyl-1-pyrazolyl)borato(phenylethanedithiodiolato)(oxo)rhenium(V) 37

2.9. COSY Experiment with Tp' Rhenium Phenylethanedithiodiolate.....38

2.10. HSQC Experiment with Tp' Rhenium Phenylethanedithiodiolate.....41

2.11. nOe Experiments with Tp' Rhenium Phenylethanedithiodiolate.....45

2.12. Determination of Dihedral Angles of the Diolate Ring of Tp' Rhenium Dithiodiolate And Monothiodiolate Complexes in Solution.....48

2.13. Recrystallization and X-ray Crystal Structure of Tp' Rhenium Dithiodiolates.....52

2.14. Attempted Cycloreversion of Tp' Rhenium Dithiodiolate and Monothiodiolate Complexes.....54

2.15. Energetics of Alkene Addition to ReS_4^-.....54

2.16. Reaction of a Rhenium Dioxo Complex and Ethylene sulfide.....61

2.17. Reaction of Rhenium Dioxo Complex and Cyclohexene Sulfide.....65

TABLE OF CONTENTS (Continued)

Page

Chapter 3. Experimental.....67

3.1. General Techniques.....67

3.2. Synthesis and Characterization of Potassium Hydrido-*tris*-(3,5-dimethyl-1-pyrazolyl)borate 67

3.3. Synthesis and Characterization of Hydrido-*tris*-(3,5-dimethyl-1-pyrazolyl)borato(trioxo)rhenium(VII).....68

3.4. General Procedure for the Thiodiolate and Dithiodiolate Synthesis.....69

3.5. Synthesis and Characterization of Hydrido-*tris*-(3,5-dimethyl-1-pyrazolyl)borato(ethane-1,2-dithiodiolato)(oxo)rhenium(V).....69

3.6. Synthesis and Characterization of Hydrido-*tris*-(3,5-dimethyl-1-pyrazolyl)borato(ethane-1,2-monothiodiolato)(oxo)rhenium(V).....70

3.7. Synthesis and Characterization of Hydrido-*tris*-(3,5-dimethyl-1-pyrazolyl)borato(ethane-1-thio-2-methyl-1,2-diolate)(oxo)rhenium(V).....71

3.8. Synthesis and Characterization of Hydrido-tris-(3,5-dimethyl-1-pyrazolyl)borato(phenylethanedithiodiolato)(oxo)rhenium(V).....72

3.9. Synthesis and Characterization of Styrene Trithiocarbonate.....74

3.10. Synthesis and Characterization of Phenylethanedithiol.....75

3.11. Reaction of Rhenium Dioxo Complex and Ethylenesulfide.....75

3.12. Reaction of Rhenium Dioxo Complex and Cyclohexene Sulfide.....77

3.13. Procedure for Recrystallization of Hydrido-*tris*-(3,5-dimethyl-1-pyrazolyl)borato(ethane-1,2-dithiodiolato)(oxo)rhenium(V).....78

TABLE OF CONTENTS (Continued)

Page

3.14. Single-Crystal X-ray Diffraction Analysis of Hydrido-*tris*-(3,5-dimethyl-1-pyrazolyl) borato(ethane-1,2-dithiodiolato) (oxo)rhenium(V).....79

3.15. Cycloreversion Reaction of Hydrido-*tris*-(3,5-dimethyl-1-pyrazolyl) borato (oxo)(dithiodiolate) and (Monothiodiolate)rhenium(V) Complexes 80

Chapter 4. Conclusions.....82

Bibliography.....83

Appendix. Crystallographic Data.....88

LIST OF FIGURES

Figure Page

1.1. Catalytic Cycle in Wacker Process.....2

1.2. Epoxidation of Ethylene Catalyzed by Silver Metal.....3

1.3. Enantioselective Epoxidation of Allylic Alcohols.....3

1.4. Mo/Co/S Cluster, Model for Homogeneous HDS Catalysts.....4

1.5. Desulfurization of ArSH by Mo/Co/S Cluster.....5

1.6. Dihydroxylation of Cyclohexene.....5

1.7. Five Membered Ring Intermediate in Dihydroxylation.....6

1.8. Concerted Mechanism for Dihydroxylation.....6

1.9. Oxametallacyclobutane Intermediate.....7

1.10. Cycloreversion of Cp* Rhenium Ethanediolate Complex.....8

1.11. Reversible Oxidation of Norbornene by Cp^*ReO_3.....9

1.12. Cycloreversion of Tp' Rhenium Ethanediolate.....11

1.13. Proposed Cycloreversion of Cp* Rhenium Ethanedithiolate Complex.....12

1.14. Fragmentation of Cp* Rhenium Ethanedithiolate.....12

1.15. Binding of Tetrathioperrhenate Anion to Norbornene.....13

1.16. Reaction of ReS_4^-, Hydrogen Sulfide, and Ethylene.....14

1.17. Structure of Tp Rhenium Ethanedithiodiolate Complex.....16

1.18. Tp Rhenium Ethanedithiodiolate Complex.....17

1.19. Synthesis of Compound **38**.....18

LIST OF FIGURES (Continued)

Figure Page

1.20. Catalytic Cycle for Deoxygenation of Epoxides.....19

1.21. Reaction between Cp'$ReCl_4$ and Alkene Sulfide.....20

1.22. A Coordinated Episulfide Intermediate.....21

2.1. Cycloreversion of Tp' Rhenium (V) Diolates.....24

2.2. Sulfur Analogs of Tp' Rhenium (V) Diolates.....24

2.3. The Simulated Spectrum and the Spectrum from ^1H NMR Experiment.....27

2.4. nOe Experiments with Tp' Rhenium Propanemonothiodiolate.....29

2.5. nOe Spectrum of *Anti*-Isomer of Tp' Rhenium Propanemonothiodiolate.....31

2.6. nOe Spectrum of *Syn*-Isomer of Tp' Rhenium Propanemonothiodiolate.....33

2.7. Synthetic Plan for the Synthesis of Phenylethanedithiol.....34

2.8. Dimerized Product from Basic Hydrolysis of Styrene Trithiocarbonate.....36

2.9. Mechanistic Explanation of Formation of Dimerized Product.....36

2.10. COSY Spectrum of Mixture of *Syn*- and *Anti*-Isomers of Tp' Rhenium Phenylethanedithiodiolate.....40

2.11. HSQC Spectrum of Tp' Rhenium Phenylethanedithiolate.....42

2.12. nOe Spectrum of Tp' Rhenium Phenylethanedithiolate.....47

2.13. Karplus Equation.....48

2.14. Karplus Equation Modified by Pachler.....49

LIST OF FIGURES (Continued)

Figure Page

2.15. Two Conformations in Solution of Tp' Rhenium Ethanedithiodiolate.....50

2.16. ORTEP from the X-ray Crystallographic Analysis of Tp' Rhenium Dithiodiolate.....52

2.17. Structures Used in DFT Calculation (LACVP** with B3LYP Functionals).....55

2.18. Heat of Reaction of Coupling of H_2S and Ethylene Additions to ReS_4^-.....56

2.19. Two Proposed Pathways for Deoxygenation.....61

2.20. Proposed Mechanism for Reaction of Rhenium Dioxo Complex and Ethylene Sulfide.....63

2.21. Formation of Tp' Rhenium Monothiodiolate Complex.....64

LIST OF TABLES

Table — Page

1.1. Selected Interatomic Distances from X-Ray Crystallographic Analysis of Compound **35**.....16

2.1. Coupling Constants of Methylene Protons from Spectrum-Matching Simulation.....26

2.2. NMR Results from HSQC Experiment.....43

2.3. List of Coupling Constants of Tp' Rhenium Ethanedithiodiolate.....49

2.4. Vicinal Coupling Constants and Calculated Average H-C-C-H Dihedral Angles.....51

2.5. Selected Bond Lengths And Bond Angles of Tp' Rhenium Ethanedithiodiolate.....53

2.6. The Energies of Minimized Structures Shown in Figure 2.18.....56

2.7. DFT Calculation of Cycloreversion of Tp' Rhenium Dithiodiolate and Monothiodiolate Complexes.....59

2.8. Comparison of Parameters from X-Ray Crystal Structure and Optimized Structure by DFT Calculation of Tp' Rhenium Ethanedithiodiolate Complex.....60

LIST OF APPENDIX TABLES

Table — Page

A.1. Crystal Data and Structure Refinement for Tp'Re(O)(SCH_2CH_2S).....88

A.2. Atomic Coordinates (x 10^4) and Equivalent Isotropic Displacement Parameters ($Å^2$x 10^3) for Tp'Re(O)(SCH_2CH_2S).....89

A.3. Bond Lengths [Å] and Angles [°] for Tp'Re(O)(SCH_2CH_2S).....90

A.4. Anisotropic Displacement Parameters ($Å^2$x 10^3) for Tp'Re(O)(SCH_2CH_2S).....93

A.5. Hydrogen Coordinates (x 10^4) and Isotropic Displacement Parameters ($Å^2$x 10^3) for Tp'Re(O)(SCH_2CH_2S).....94

Synthesis, Characterization, and Reactivity of Rhenium Dithiodiolate and Monothiodiolate Complexes

Chapter 1. Introduction and Literature Review

1.1 Formation of C-O and C-S Bond By Transition Metal Complexes

Formation of C-O bonds is an important process for organic synthesis and industrial purposes due to the extensive application to several chemical transformations. This process can be catalyzed by a range of transition metal complexes. One of the useful applications is the Wacker process for oxidation of ethylene to acetaldehyde[1]. Acetaldehyde is a major intermediate for production of acetic acid and other useful chemicals[2]. In this process, ethylene is oxidized by using palladium chloride (Pd^{2+}). Basically, palladium chloride has to be a stoichiometric reagent for this process. However, copper chloride (Cu^{2+}) is used in order to reoxidize Pd^{o} to Pd^{2+}; Oxygen also gets involved by reoxidizing Cu^{+} to Cu^{+2}, and the catalytic cycle can be completed (Figure 1.1).

Another example for C-O formation is the epoxidaiton reaction. Transition metal catalyzed epoxidation reactions have been widely used[3,4], and the stoichiometric oxidant can be molecular oxygen. For example, ethylene glycol synthesis can be performed by using silver metal as a catalyst and molecular oxygen as a stoichiometric oxidant[5].(Figure 1.2) Some of other transition metal complexes, such as molybdenum compounds, also have activity as catalyst for

epoxidation[6]. Vanadium alkylperoxide complexes can also be an alternative to stoichiometric reagents for epoxidation[7].

Figure 1.1: Catalytic Cycle in Wacker Process

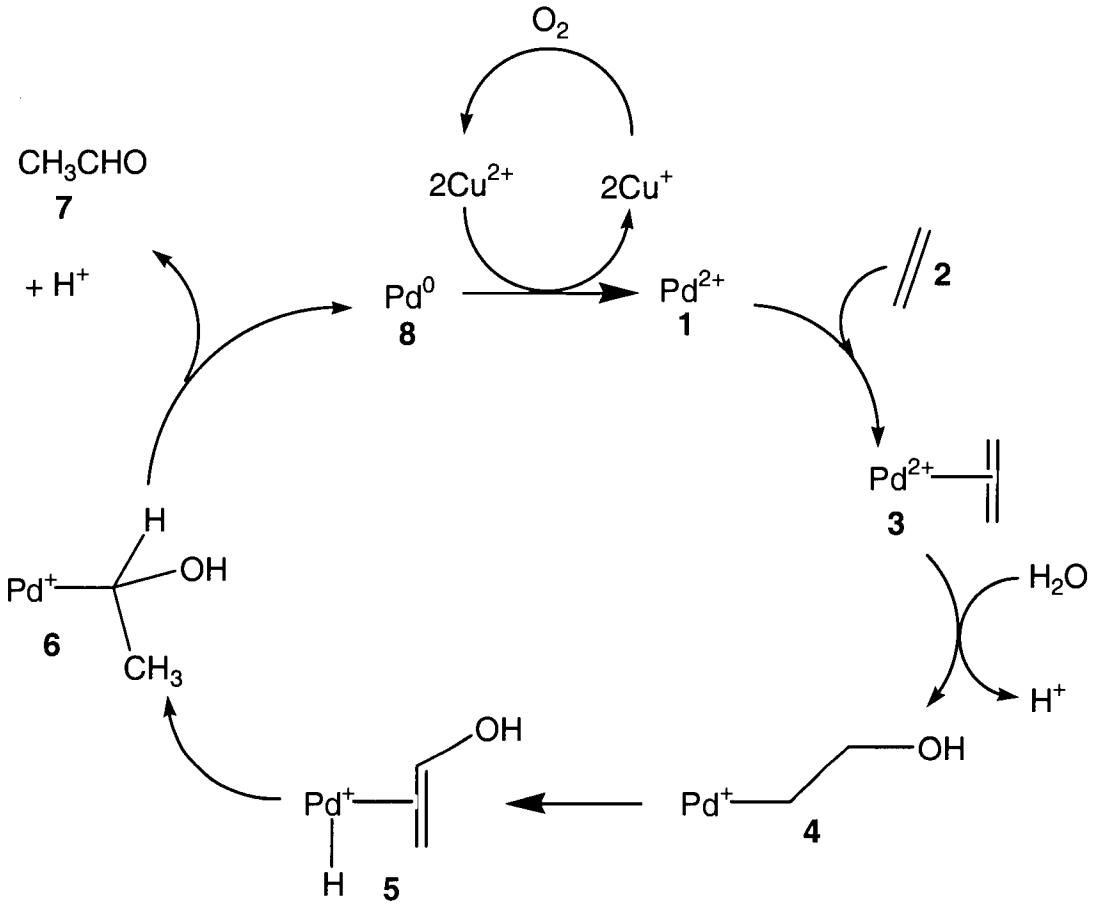

Figure 1.2 Epoxidation of Ethylene Catalyzed by Silver Metal

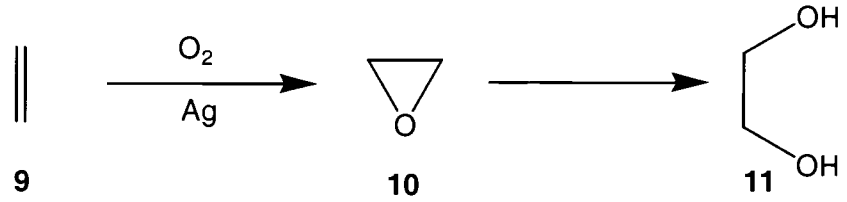

Sharpless asymmetric epoxidation is the asymmetric version of epoxidation for allylic alcohols by using t-butyl hydroperoxide, enantiomerically pure tartrate esters, and titanium tetraisopropoxide[8]. This reaction can be done with catalytic amounts of titanium isopropoxide and the tartrate ester[9]. Removal of water by molecular sieves has an effect on both the rate and enantioselectivity of the reaction. (Figure 1.3)

Figure 1.3 Enantioselective Epoxidation of Allylic Alcohols[10]

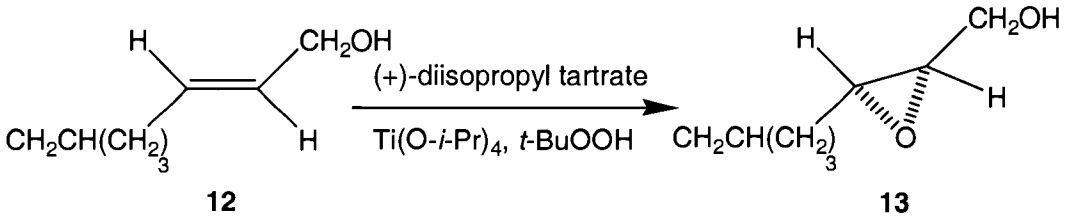

Formation of the C-S bond is also active research topic due to extensive applications in the petrochemical industry. Study on C-S bond-break and bond-making reactions will provide some mechanistic details needed for development of the catalyst for hydrodesulfurization process (HDS), which is the removal of sulfur

from the petroleum feedstocks by using catalyst and hydrogen gas[11]. The products of this process will be hydrocarbons and H_2S; the latter can be disposed of as elemental sulfur by Claus process[12]. Hydrodesulfurization (HDS) of fossil fuels is also an important process to the preservation of environmental quality due to the fact that combustion of sulfur-containing compounds provides sulfur oxides that contribute to acid rain when combined with atmospheric water[13].

Homogeneous S-atom abstraction reactions of Mo/Co/S clusters have been studied as an ideal model of hydrodesulfurization process[14]. The structures of Mo/Co/S clusters are shown in Figure 1.4, and an example of desulfurization by using Mo/Co/S clusters are demonstrated in Figure 1.5. The mechanistic investigation of this process is an active research area.

Figure 1.4: Mo/Co/S Cluster, Model for Homogeneous HDS Catalysts

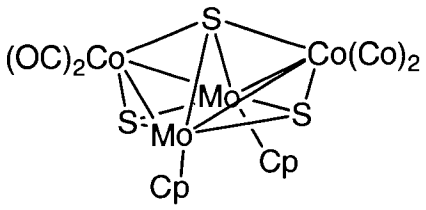

12

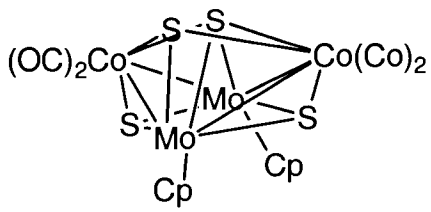

13

Figure 1.5: Desulfurization of ArSH by Mo/Co/S Cluster

1.2 Dihydroxylation of Olefins by OsO_4 and Mechanistic Study

Effective reagents for dihydroxylation of olefins are permanganate ion and osmoim tetroxide[15]. By using these reagents, diols are formed by syn addition. The disadvantages of using osmium tetroxide are that it is quite expensive and molecular oxygen cannot generally be used as an oxygen source for the oxidation although a recent paper showed this[64]. However, these drawbacks one can be minimized by procedures that use only a catalytic amount of osmium tetroxide. An amine oxide, such as N-methylmorpholine-N-oxide (NMO), can be used as the stoichiometric oxidant[16]. An example of this type of reaction is shown in Figure 1.6 as a dihydroxylation of cyclohexene.

Figure 1.6: Dihydroxylation of Cyclohexene

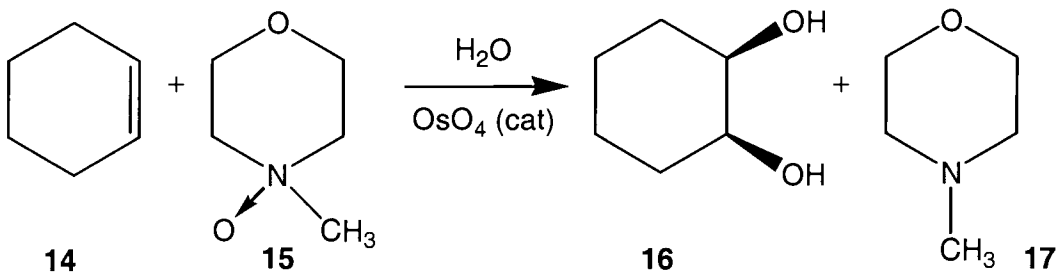

The mechanism of this reaction involves the formation of a 5 membered ring intermediate shown in Figure 1.7. This reaction is a first order kinetics for olefins and also first order for osmium tetroxide. Alkenes are nucleophile in this reaction due to the fact that electron rich alkenes react faster than electron deficient alkenes[17]. There are controversies concerning the mechanism of this process. Criegee[18] and Corey[19] believe that it proceeds through the classic concerted mechanism shown in Figure 1.8. This mechanism is consistent with the syn addition product, but this type of pericyclic mechanism is not known for any reaction involving a transition metal.

Figure 1.7: Five Membered Ring Intermediate in Dihydroxylation

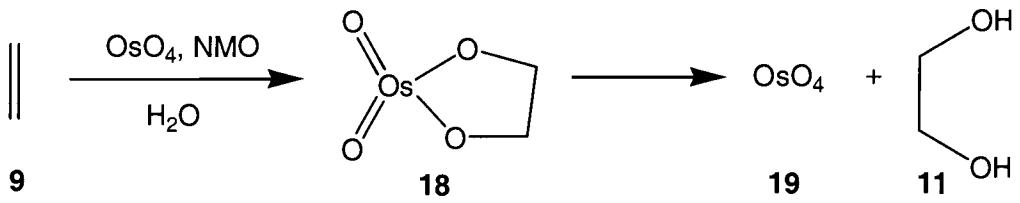

Figure 1.8: Concerted Mechanism for Dihydroxylation

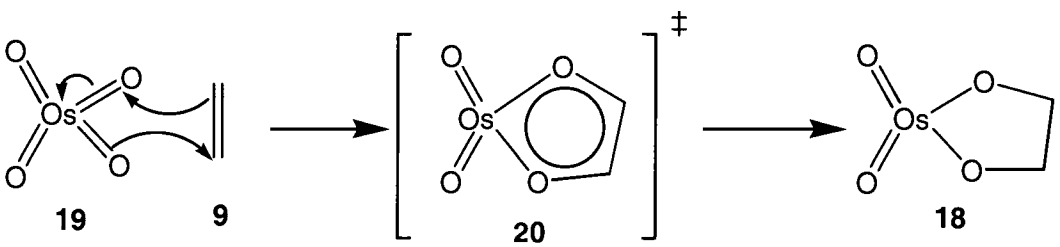

In 1977, Sharpless[20] proposed the stepwise mechanism involving the oxametallacyclobutane intermediate shown in Figure 1.9. In this mechanism, the enantioselectivity can be explained by the effect of the steric effect between bulky ligand and the oxametallacyclobutane. However, there were some theoretical works supported the concerted [3+2] mechanism[21]. The mechanism of dihydroxylation by osmium tetroxide is still an active research.

Figure 1.9: Oxametallacyclobutane Intermediate

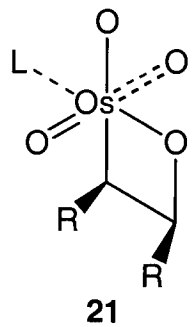

21

1.3 Use of Rhenium Diolates for Study of Dihydroxylation Reaction of Olefins

The Gable group has worked on rhenium diolates in different aspects. One of them is to study on cycloreversion reaction. From the principle of microscopic reversibility[22], this study would provide useful mechanistic information for dihydroxylation reaction of olefins due to the fact that the cycloreversion reaction is the microscopic reverse of dihydroxylation reaction. In 1987, Herrmann reported

the cycloreversion reaction of Cp* rhenium ethanediolate complex (Cp* = pentamethylcyclopentadienyl). This process is shown in Figure 1.10. The same process also occurs in the rhenium diolate containing the hydrido-*tris*-pyrazolyl borate (Tp) ligand[65].

Figure 1.10: Cycloreversion of Cp* Rhenium Ethanediolate Complex

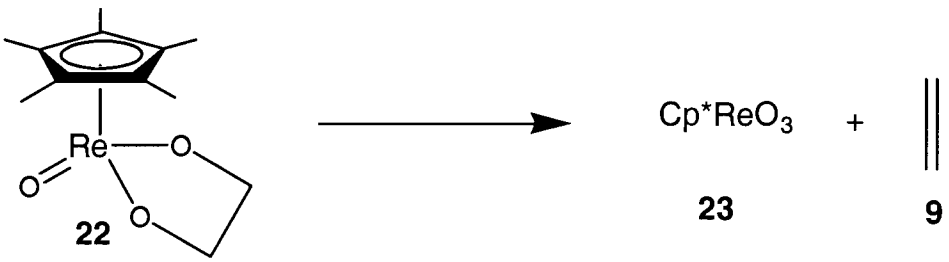

1.4 Cycloreversion of Cp* Rhenium (V) Diolates

In 1993, Gable[23] reported the kinetics of reversible oxidation of norbornene by Cp^*ReO_3. Norbornene was allowed to react with Cp^*ReO_3 in deuterated benzene in sealed tube at 90-125 °C. Formation of two diolates, which were syn and anti products, in equilibrium with the reactants was observed (see Figure 1.11) even a 10-fold or greater excess of norbornene were used. The result suggested that the cycloreversion is an entropically driven process. The equilibrium constant was determined to be 11.4(1.5) at 122.4 °C. The effect of strain in the alkene was also reported in 1994 by Gable[24]. The kinetics extrusion and oxidation of ethylene, 2-butene, and norbornene were measured. The calculated activation parameters

shown a large effect arouse from strain in the double bond of alkenes. On the other hand, strain in the double bond has a very small or no effect on alkene extrusion.

Figure 1.11: Reversible Oxidation of Norbornene by Cp^*ReO_3

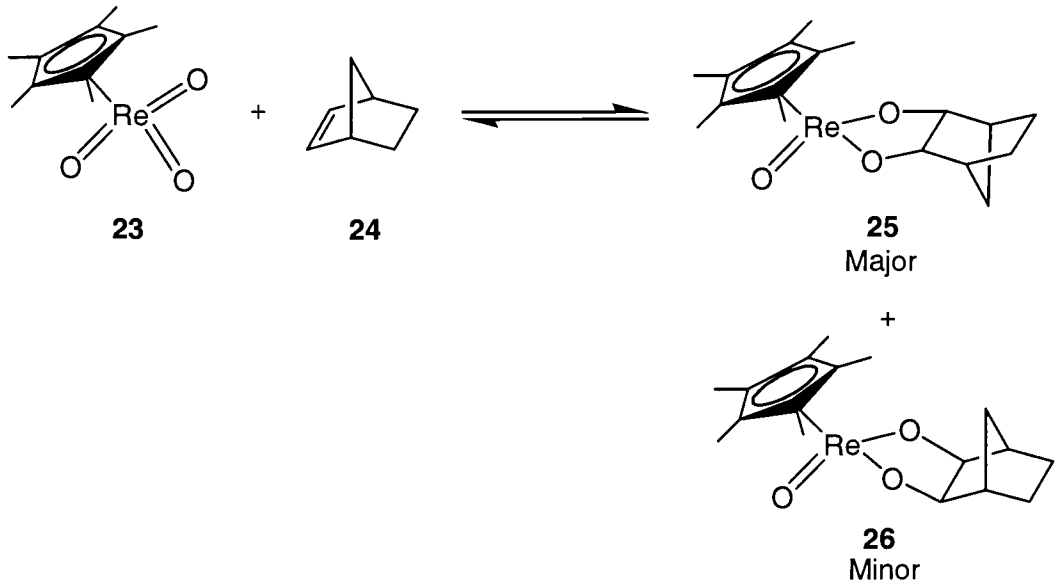

The effect of substitution and conformation on the cycloreversion reaction of Cp* rhenium diolates has also been investigated. Gable also shown that methyl group substitution on the diolate ring increases the activation enthalpy of this process[25]. In this experiment, the kinetics of extrusion of different alkenes from Cp* rhenium diolates were measured, and some activation parameters were calculated. The solution conformation of all Cp* rhenium diolate complexes used in this experiment was also analyzed by using a Karplus relationship between vicinal coupling constants and dihedral angles.

From the conformational analysis and calculated activation parameters, the staggered geometry of the diolate ring causes the entropy of activation to become more positive, and increase the rate of extrusion. These rate changes are independent of electronic and steric substituent effects. This observation is consistent with a stepwise mechanism, which is the formation of a metallaoxetane by migration of carbon from oxygen to rhenium.

In another study, Gable performed the Hammett studies on alkenes extrusion from rhenium (V) diolates[26]. Cp* rhenium phenylethane-1, 2-diolate exhibits a linear relationship with Hammett σ- constants, with $\rho = 0.42$. The substituents on the phenyl group of these diolates included *p*-methoxy, *p*-methyl, *p*-fluoro, *p*-chloro, *p*-trifluoromethyl, and *m*-nitro. The slope of 0.42 suggested an increase in electron density at the benzylic carbon. This result is also consistent with the formation of metallaoxetane by alkyl migration from oxygen atom to rhenium.

1.5 Cycloreversion of Tp' Rhenium (V) Diolates

The Tp' ligand has been known to act as a "cyclopentadienyl equivalent." Namely, it is an anionic, six-electron donor, which is the same as Cp* ligand. Consequently, similar chemistry such as cycloreversion should be observed in the case of the Tp' rhenium diolate. In 1999, Gable and co workers reported that rhenium (V) diolate with Tp' ligand (Tp' = hydrido-*tris*-(3.4-

dimethylpyrazolyl)borate) also cyclorevert to $Tp'ReO_3$ and alkenes[27]. The reaction for Tp' rhenium ethanediolate is shown in Figure 1.12.

Figure 1.12: Cycloreversion of Tp' Rhenium Ethanediolate

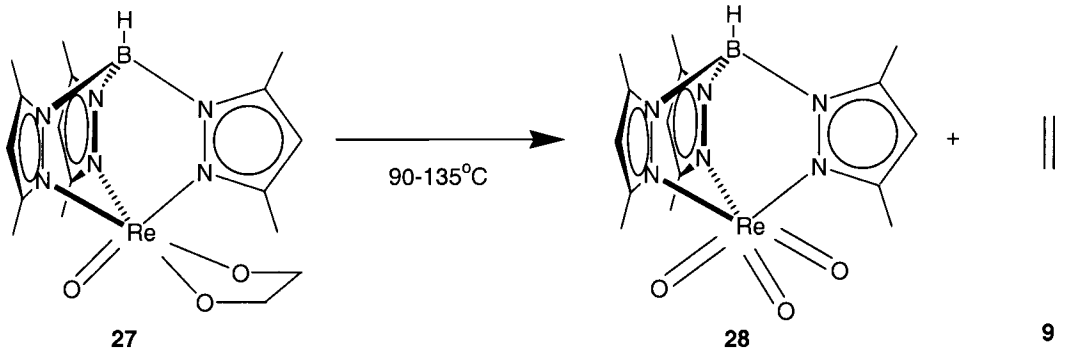

27 28 9

All of the rhenium diolate work leads to the question whether or not the sulfur analogs, which are the rhenium dithiodiolate and monothiodiolate, will exhibit the same cycloreversion reactivity. Should such reactivity be observed, this investigation will also provide important mechanistic and thermodynamic evidence about the cycloreversion reaction, which may be comparable to the work done in diolate systems.

1.6 Report of Alkenes Extrusion from Cp* Rhenium (V) Dithiodiolate

Herrmann reported extrusion of ethylene from Cp* rhenium ethanediolate (**22**). The sulfur analog of diolate (**22**), which is ethanedithiodiolate (**29**), was also

synthesized and appeared to be thermally more stable than the diolate complex. However, a quantitative loss of ethylene from Cp* rhenium ethanedithiodiolate upon heating (see Figure 1.12) at 200 °C over 30 minutes was observed. It may be hard to draw a conclusion that ethylene observed in this process comes from the cycloreversion reaction of ethanedithiodiolate (**29**) due to the fact that none of the rhenium species was characterized. Presumably, ethylene produced in this process could either be a product of cycloreversion (Figure 1.13) or a product from multistep fragmentation shown in Figure 1.14.

Figure 1.13: Proposed Cycloreversion of Cp* Rhenium Ethanedithiolate Complex

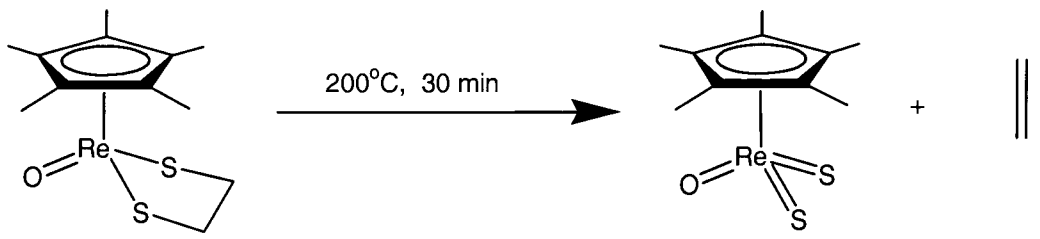

Figure 1.14: Fragmentation of Cp* Rhenium Ethanedithiolate

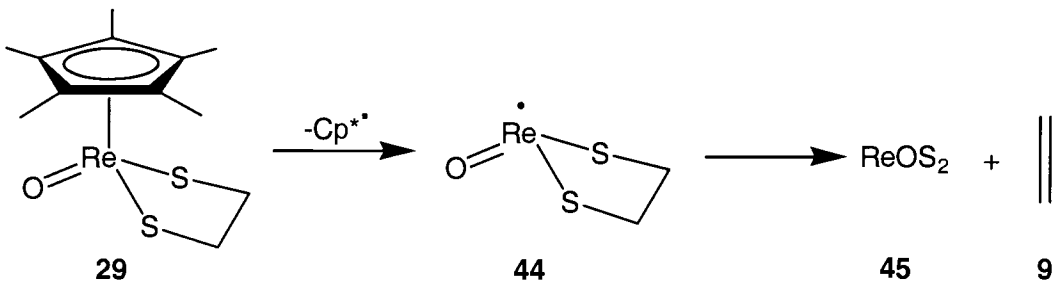

1.7 Binding of Alkene to Tetrathioperrhenate Anion (ReS_4^-) and Influence of Hydrogensulfide and Thiols

Tetrathioperrhenate anion, ReS_4^- (**31**), is isoelectronic with OsO_4, and it reacts with alkenes[28]. In 1999, Rauchfuss reported that ReS_4^- reversibly binds alkenes[29]. The binding of ReS_4^- to norbornene was studied (see Figure 1.15).

Figure 1.15: Binding of Tetrathioperrhenate Anion to Norbornene

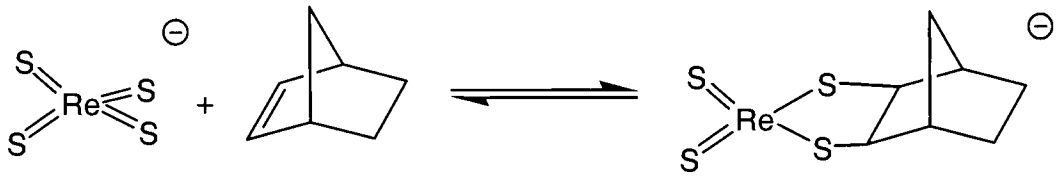

31 **24** **32**

ReS_4^- and norbornene were allowed to react in acetonitrile at 23 °C, and the reaction was monitored by UV-VIS spectroscopy because tetrathioperrhenate anion (**31**) and the adduct (**32**) have a different maximum absorptions at around 508 nm and 440 nm respectively. Plots of [ReS_4^-] vs [adduct]/[norbornene] were linear with a slope of K_{eq}^{-1}. For the reaction between ReS_4^- and norbornene, K_{eq} is about 9400 M^{-1} at 23 °C in acetonitrile. The equilibrium constant also reflected a solvent dependence when different solvents were used, but the result did not correlate with dielectric constant of the solvent.

The determination of thermodynamic parameters was performed by evaluating K_{eq} over the range of 5-50 °C. Plot of $\ln(K_{eq})$ vs T^{-1} were linear, providing the thermodynamic values as follow: ΔH^{o} = -12.67 kcal-mol^{-1} and ΔS^{o} = -23.44 cal-mol^{-1}K^{-1}.

Binding of ReS_4^- to norbornene appeared to be a favorable process due to a high equilibrium constant observed at 23 °C in acetonitrile solution. The influence of hydrogen sulfide and thiols on the binding of alkenes to ReS_4^- was also investigated[30]. Reaction of ReS_4^-, hydrogen sulfide, and alkenes yielded the rhenium (V) derivatives, $Re(S)(S_2(alkene))(SH)_2^-$. These adducts were formed by the addition of hydrogen sulfide to intermediate dithiodiolates. The reaction in which ethylene was used as alkene is shown in Figure 1.16.

Figure 1.16: Reaction of ReS_4^-, Hydrogen Sulfide, and Ethylene

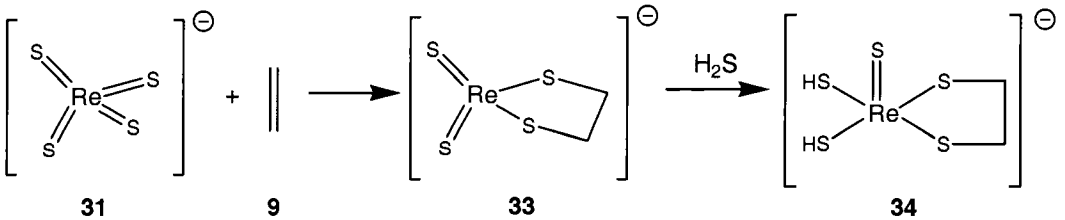

31 **9** **33** **34**

The first step was reported to be favorable with a high equilibrium constant. The second step is even more favorable due to a greater stability of adduct **33**. Alkene adducts, such as adduct **33**, also reacted with thiols yielding the same type of products, which were more stable. The stabilization of the adduct resulting from

addition of hydrogen sulfide or thiols to dithiodiolate adduct can be explain by the spectator sulfido effect, which states that "Addition of RSH across a Re=S bond provides the very stabilizing X_4Re^V=S species". This idea originated from the spectator oxo effect, which was a result from the theoretical study from Rappe' and Goddard in 1982[31]. Quantum chemical calculation from their work shown that tetrahedral complexes of M(=E)(=E')X_2 bind to several reagents to give d^2 square pyramidal derivatives. This process was driven by formation of one strongly bonded terminal M=E, where E = O, NR, unit. Coucouvanis has applied this idea to explain the reactivity of tetrahedral species containing sulfide ligand[32]. In this experiment of Rauchfuss, this concept is also applicable for explanation of stability of the addition adduct.

1.8 Sturctures and Synthesis of Tp Rhenium Ethanedithiodiolate Complex

Tp rhenium ethanedithiodiolate (Tp = hydrido-*tris*-(pyrazolyl)borate) was synthesized and the crystallographic analysis was also reported in 1993 [33]. According to this report, compound **35** (see Figure 1.18) was synthesized by reaction of TpRe(O)Cl_2, triethylamine, and ethanedithiol. The reaction was done at reflux temperature of ethanol for 4 hours. The brown microcrystalline solid of compound **35** was then recrystallized from methylene chloride/ethanol. The red-brown crystals were obtained and analyzed by X-ray crystallographic technique. Selected interatomic distances are shown in Table 1.1.

Table 1.1: Selected Interatomic Distances from X-Ray Crystallographic Analysis of Compound **35**

	(Angstrom)		(Angstrom)
Re-O	1.694(9)	Re-N_5	2.14(1)
Re-S_1	2.280(4)	Re-N_3	2.17(1)
Re-S_2	2.299(4)	Re-N_1	2.31(1)

Figure 1.17: Structure of Tp Rhenium Ethanedithiodiolate Complex **(35)**

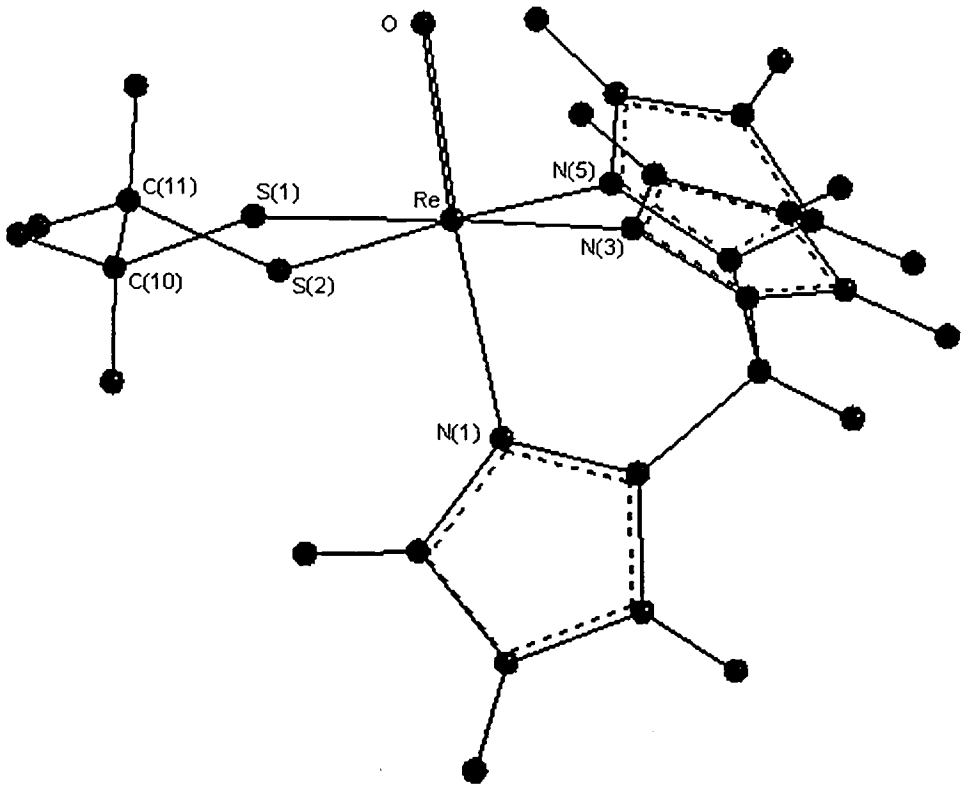

Figure 1.18: Tp Rhenium Ethanedithiodiolate Complex **(35)**

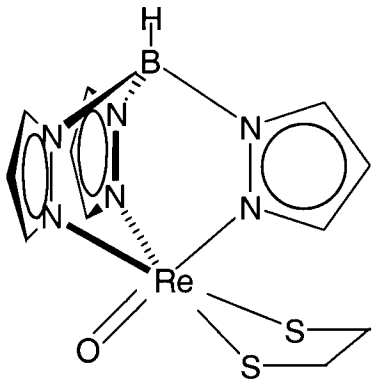

35

From the structure of compound **35** (Figure 1.17) and table 1.1, rhenium atom is in a distorted octahedral environment. The Re-N_1 bond distance is longer than the other two Re-N bonds due to the fact that N_1 is trans to Re-O bond, hence experiences the trans effect. Three pyrazole rings appear to be planar, while five membered dithiodiolate ring exhibits an envelope form with C_{11} displaced by 0.620 angstrom above the mean plane of the other four atoms. The diagnostic IR Re=O bond vibration for this compound was reported to be 951 cm^{-1}.

Some of dithiodiolato(oxo)rhenium (V) complexes were also synthesized and characterized by X-ray crystallographic technique. $CH_3Re(O)(SCH_2CH_2S)PPh_3$ **(38)** was synthesized by reacting methyloxorhenium (V) complex with two monodentate thiolate ligands **(36)** with ethanedithiol **(37)**[34]. This reaction is shown in figure 1.19. The crystals of compound **38** were obtained by recrystallization in dichloromethane. The Re-S bond distances of compound **38** are very similar to the

distances in compound **35**. Namely, Re-S bond distances are 2.2870(8) and 2.2915(8) angstrom for compound **38** and 2.280(4) and 2.299(4) angstrom for compound **35**. The Re-O bond of compound **38** is a little bit shorter than the Re-O bond in compound **35,** namely, 1.681(2) compare to 1.694(9) angstrom.

Figure 1.19: Synthesis of Compound **38**

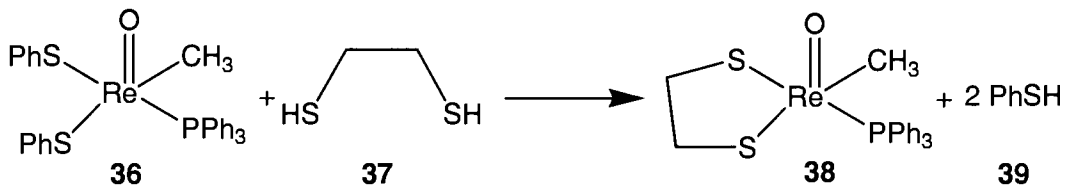

1.9 Catalytic Deoxygenation of Epoxides Using Tp' Rhenium Oxide

In 2000, Gable reported the catalytic deoxygenation of epoxides by using Tp' rhenium oxide species[35]. In this process, the dioxo species were responsible for transferring oxygen atom from epoxide to triphenylphosphine, which was a stoichiometric reductant. The kinetics of this process was also monitored by using ^{1}H NMR spectroscopy. The first step of this process was the in situ reduction of Tp'ReO_3 by triphenylphosphine yielding the dioxo species. This species then reacted with epoxide giving alkene and Tp'ReO_3 as products. The catalytic cycle is shown in figure 1.19. Only the catalytic amount of Tp'ReO_3 (1-5 mol%)was needed in order to run this process, and high yields of alkene were obtained. From the kinetic study of this process, electronic and steric factors arising from epoxides

played an important role on the rate of oxygen atom transfer. Namely, *cis*-alkenes reacted faster than *trans*-alkenes. Epoxides of terminal alkenes reacted faster than those of internal alkenes. Alkyl substituted epoxides reacted slower than aryl stubstituted epoxide. Some functional groups, such as hydroxyl and nitro groups, were shown to interfere with the catalyst. The presence of water also inhibited the catalytic turnover. The Tk rhenium trioxide (Tk = *tetrakis*-pyrazolylborate) was also used in this experiment. However, the rate of reaction with Tk rhenium trioxide was significantly retarded compare to Tp' rhenium trioxide.

Figure 1.20: Catalytic Cycle for Deoxygenation of Epoxides

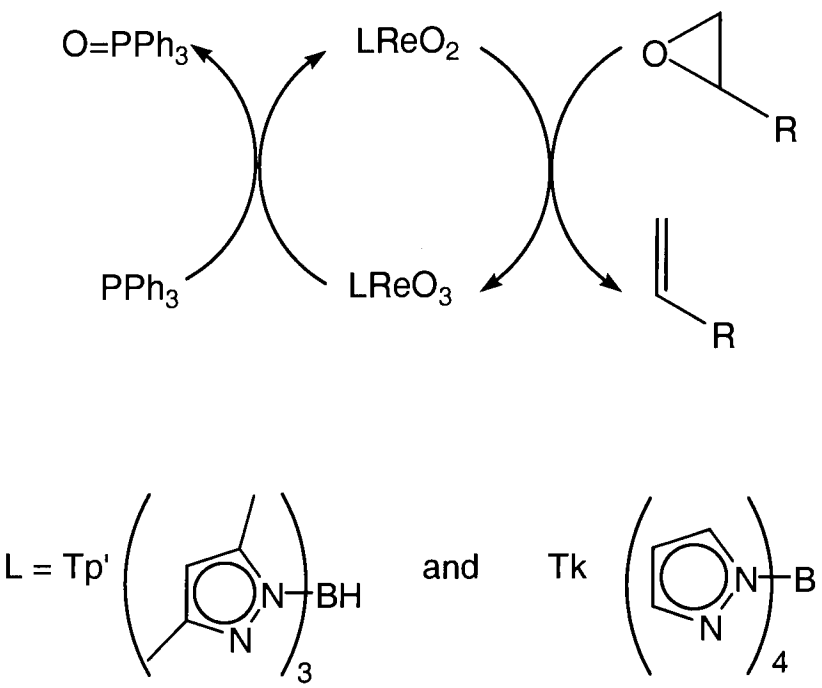

1.10 Reaction of Ethylene Sulfide and Propylene Sulfide with $Cp'ReCl_4$ Complex

Dubois reported the reaction of $Cp'ReCl_4$ **(40)** with ethylene sulfide and propylene sulfide[36]. The $Cp'ReCl_4$ complex was allowed to react with excess ethylene sulfide at room temperature. A rapid color change from red to intense purple was seen. The same color change was observed when propylene sulfide was used. This reaction is shown in Figure 1.21.

Figure 1.21: Reaction between $Cp'ReCl_4$ and Alkene Sulfide

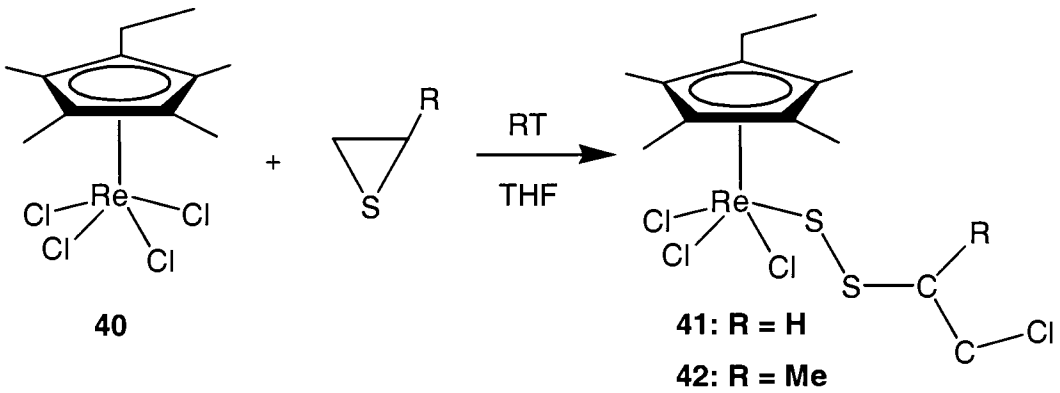

Compound **42** was recrystallized in a dichloromethane/pentane solution, and the X-ray crystallographic analysis was performed. Attempts to determine the sequence of the reaction steps of formation of compound **41** and **42** were done. $Cp'ReCl_4$ was allowed to react with 1 equivalent of propylene sulfide at room temperature. The product NMR spectrum shown a 1:1 ratio of $Cp'ReOCl_2$ and compound **42**. $Cp'ReCl_4$ was also allowed to react with excess ethylene sulfide in a

nonpolar solvent (deuterated benzene or toluene), and the reaction was monitored by NMR spectroscopy both at room temperature and –45 °C. Interestingly, at low temperature, the formation of a red intermediate was observed. A ^{13}C NMR of this intermediate showed a single carbon resonance of the coordinated ligand, which, in this case, is a characteristic of C_s symmetry. This observation indicated that this intermediate species does not contain a ring-opened episulfide. The intermediate complex is assigned to be a coordinated episulfide **43** shown in figure 1.22.

Figure 1.22: A Coordinated Episulfide Intermediate

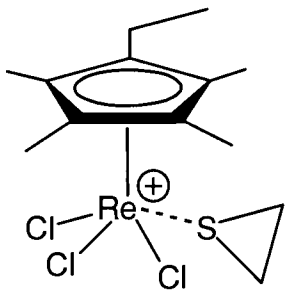

43

From the information obtained, Dubois proposed that, presumably, these two compounds were formed by a chloride-assisted ring opening of a S-coordinated episulfide followed by an insertion of an additional sulfur atom yielding Re-S-S-R linkage. However, the sequence of these steps is still unknown.

1.11 Conclusions of the Literature Review

According to the observation reported by Herrmann that ethylene is produced from thermolysis of the Cp* rhenium dithiodiolate complex, Tp' rhenium dithiodiolate should exhibit the same reactivity. However, thermodynamic data from the cycloaddition reaction of alkene to tetrathioperrhenate anion reported by Rauchfuss indicates that formation of dithiodiolate complex is a favorable process with a high equilibrium constant. These two observations lead to the investigation of reactivity of the Tp' rhenium dithiodiolate. The effect of having one sulfur vs two sulfur atoms toward the reactivity of these complexes can be determined by investigating the reactivity of Tp' rhenium monothiodiolate. Presumably, there is a progressive change in reactivity with each sulfur substitution. From several works reported by the Gable group, substituents on the diolate ring play an important role on the reactivity of Tp' rhenium diolate complexes. It is worthwhile to examine what effect substituents will show in case of Tp' rhenium dithiodiolate and monothiodiolate complexes. The deoxygenation of epoxides by a Tp' rhenium dioxo species also leads to the investigation of the same type of reaction with episulfides.

Chapter 2. Results and Discussion

Carbon sulfur bond formation and breaking is a key process for hydrodesulfurization (HDS). This process is catalyzed by metal sulfides, such as MoS_x/CoS_y. However, sulfides of rhenium, ruthenium, and other metals are even more active[37]. Consequently, rhenium sulfur chemistry has been investigated as homogenous catalyst for HDS process.

Alkene sulfidation, which is a reverse process of cycloreversion of dithiodiolates, was extensively study by Rauchfuss, and tetrathioperrhenate anion was used[29, 30]. This process appeared to be thermodynamically favorable when norbornene was used as alkenes. Investigation of cycloreversion of rhenium (V) dithiodiolate or monothiodiolate complexes will provide mechanistic implications for alkene sulfidation, which is an active research area due to the importance in petroleum industry. Moreover, this study will also provide mechanistic information applicable to cycloreversion of diolate complexs, the oxygen analog of dithiodiolate or monothiodiolate complexes.

2.1 Cycloreversion of Rhenium Diolates

The previous work in the Gable group reveal the cycloreversion of rhenium (V) diolates containing the hydrido-*tris*-(3,5-dimethylpyrazolyl)borate (Tp') ligand in nonpolar solvents.

Figure 2.1: Cycloreversion of Tp' Rhenium (V) Diolates

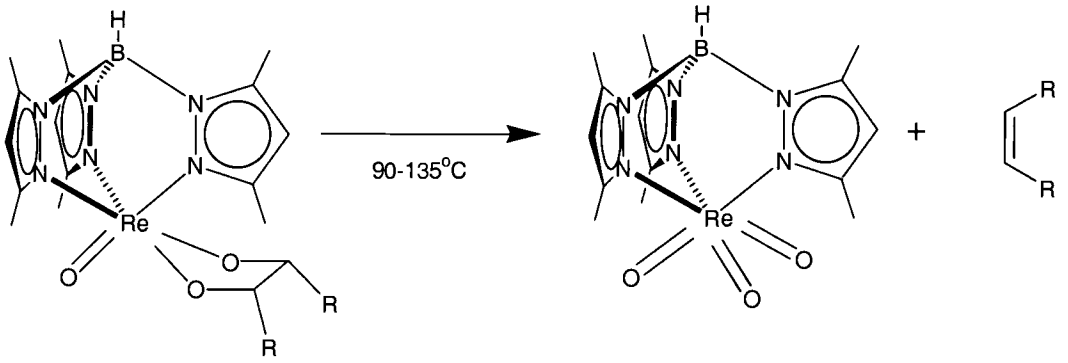

In order to investigate cycloreversion reactions of sulfur analogs of Tp' rhenium (V) diolates, first of all, the syntheses of a series of compounds must be completed. The rhenium dithiodiolate and monothiodiolate, which are shown below, were synthesized according to the previous methodology[38].

Figure 2.2: Sulfur Analogs of Tp' Rhenium (V) Diolates

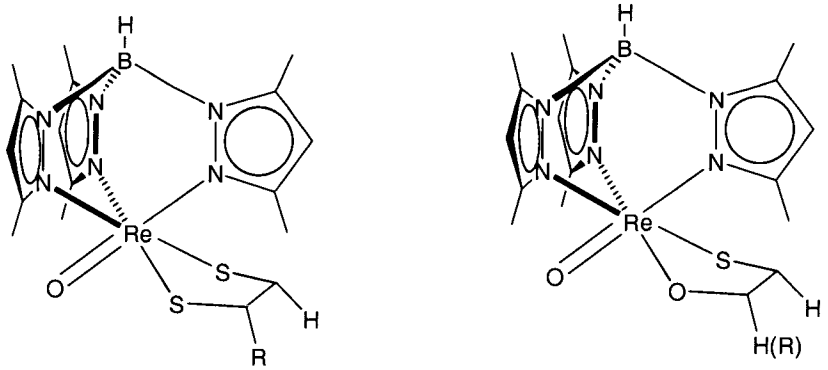

R = H **(44)**

Ph **(45)**

R = H **(46)**

CH_3 **(47)**

2.2 Synthesis and Characterization of Hydrido-*tris*-(3,5-dimethyl-1-pyrazolyl)borato(ethane-1,2-dithiodiolato)(oxo)rhenium(V) (44)

The ethanedithiodiolate was synthesized according to a one-pot procedure. The synthesis started with reduction of Tp'ReO_3 to give the dioxo species, followed by condensation with ethane-1,2-dithiol. After filtration, the solvent was removed by rotary evaporator. The crude product was then purified by column chromatography. The dark brown product was characterized by using ^1H NMR, ^{13}C NMR, IR, and mass spectrometry. The integration ratio of 1:2 for vinylic protons and 6:6:3:3 for methyl protons from Tp' shown the C_s symmetry of this complex. An infrared band at 941.53 belonged to the Re=O stretch, and mass spectrometry shown a M^+ ion at 592 m/z. However, 4 methylene protons in dithiodiolate ring at 3.59 and 4.10 ppm exhibit the AA'BB' splitting pattern, which is a second order spectrum. Consequently, not all of the coupling constants can be measured directly from the spectrum.

However, using simulation methodology allows solution of this problem. In this experiment, the spectrum simulation was performed by NUTS program. In order to get the best result, it is crucial to get start with good estimated values for all of the coupling constants. Some of those numbers can be obtained by analyzing the AA'BB' splitting pattern. The approximation of those coupling constants can be done according to the predicted pattern for spin systems with four nuclei[39]. The optimized coupling constants from spectrum-matching experiment is shown below:

Table 2.1: Coupling Constants of Methylene Protons from Spectrum-Matching Simulation

H	Chemical shift (ppm)	Coupling constant (Hz)
1	4.0987	-
2	4.0994	J (1,2) = 6.8772
3	3.5918	J (1,3) = -12.1644
		J (2,3) = 5.9523
4	3.5924	J (1,4) = 7.4167
		J (2,4) = -11.9611
		J (3,4) = 7.5388

The simulated spectrum (figure 2.3) shows a perfect matching in both intensity and splitting pattern of all peaks in methylene signals.

Figure 2.3: The Simulated Spectrum and the Spectrum from ^{1}H NMR Experiment

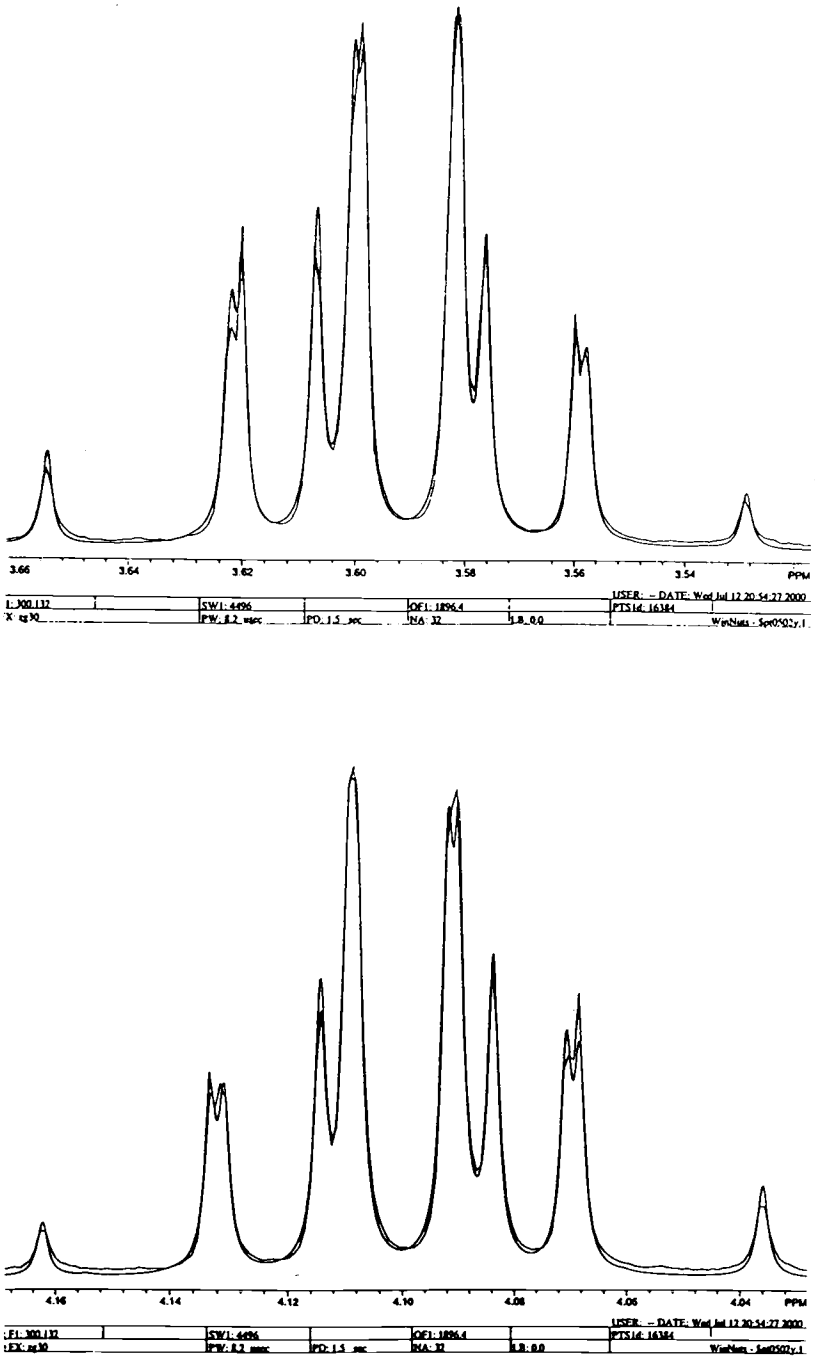

2.3 Synthesis and Characterization of Hydrido-*tris*-(3,5-dimethyl-1-pyrazolyl)borato(ethane-1,2-monothiodiolato)(oxo)rhenium(V) (46)

The analog of Tp' rhenium (oxo) diolate containing only one sulfur atom in the diolate ring was also synthesized. The first step is reduction of Tp' rhenium trioxo complex to the dioxo species followed by condensation of dioxo complex and mercaptoethanol with acid catalyst. This reaction was driven to the completion by removal of water by using freshly ground molecular sieves. These two steps were performed in one-pot fashion. The resulting blue solution was filtered. After filtration, the solvent was removed and chromatographed by using 1:1 dichloromethane/hexane as a mobile phase. The dark blue product, which was hydrido*tris*(3,5-dimethyl-1-pyrazolyl)borato(1-thioethane-1,2-diolato)(oxo) rhenium(V), was characterized by using ^{1}H NMR, ^{13}C NMR, IR, and mass spectrometry. All of the coupling constants from the methylene units of this compound can be directly extracted from the spectrum, which was collected in deuterated benzene. These coupling constants were used in the conformational analysis of this compound in solution phase, which will be described at the end of this chapter. Several attempts were made in order to recrystallize this compound from a range of solvent systems. However, none yielded X-ray quality crystals.

2.4 Synthesis and Characterization of Hydrido-*tris*-(3,5-dimethyl-1-pyrazolyl)borato(propanemonothiodiolato)(oxo)rhenium(V) (47)

Synthesis of the Tp' rhenium propanemonothiodiolate complex was accomplished by using the same one-pot procedure, which was described earlier in this chapter. After 15 hours, the reaction was filtered and the blue solution was then evaporated by using rotary evaporator. The dark blue solid product was purified by means of chromatography with1: 1 dichloromethane/hexane was used as an eluent. Two isomers of this compound were isolated as separate bands. These two compounds were fully characterized by using ^{1}H NMR, ^{13}C NMR, IR, and mass spectrometry. The nOe experiments were performed in order to distinguish between these two isomers.

Figure 2.4: nOe Experiments with Tp' Rhenium Propanemonothiodiolate

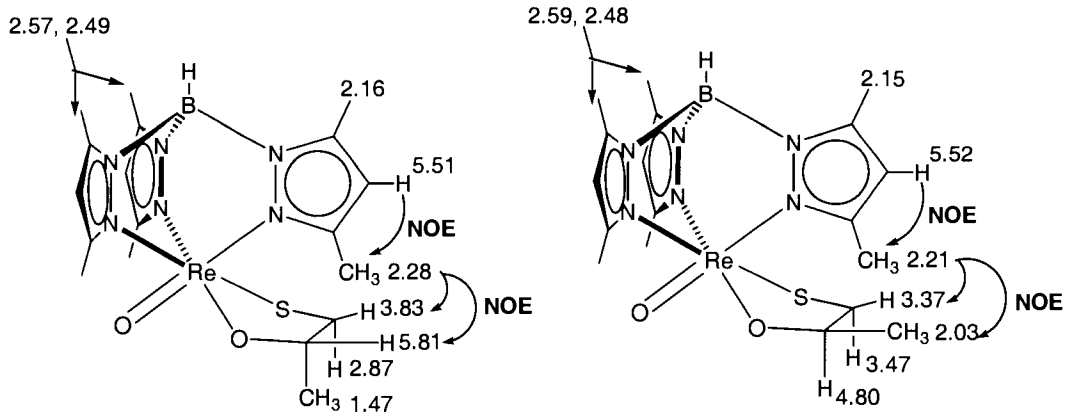

Anti-Isomer **Syn-Isomer**

2.5 nOe Experiment with *Anti*-Isomer of Tp' Rhenium Propanemonothiodiolate

An NMR sample was first irradiated at 5.51 ppm, which was a pyrazole vinylic signal. Correlation peaks were observed at 2.28 and 2.16 ppm, which are nearby methyl signals. The second irradiation was performed at 2.16 ppm, and enhanced peaks were observed at 2.57 and 2.49 ppm, which belonged to methyl groups, and 5.51 ppm, which was the peak that was irradiated at the first time. The second irradiation indicated that the signal at 2.16 ppm belonged to the methyl group that was located on the opposite side of monothiodiolate ring. The third irradiation at 2.28 ppm gave three correlation peaks at 5.51 ppm, which was a vinylic signal irradiated at the first time, 5.81 ppm, which was a methine proton on carbon bearing methyl group and oxygen atom, 3.83, which was one of the methylene protons on monothiodiolate ring. The last irradiation indicated that methyl group on the monothiodiolate ring of this compound should be pointing away from pyrazole ring. Due to the fact that correlations between one of methyl groups on the pyrazole ring and proton signals from monothiodiolate ring were observed, the pyrazole ring that we chose for the first irradiation should be located right above monothiodiolate ring. From all of the information above, this isomer was assigned to be anti-isomer. The nOe Spectrum of Anti-Isomer of Tp' rhenium propanemonothiodiolate is shown in Figure 2.5.

Figure 2.5: nOe Spectrum of *Anti*-Isomer of Tp' Rhenium Propanemonothiodiolate

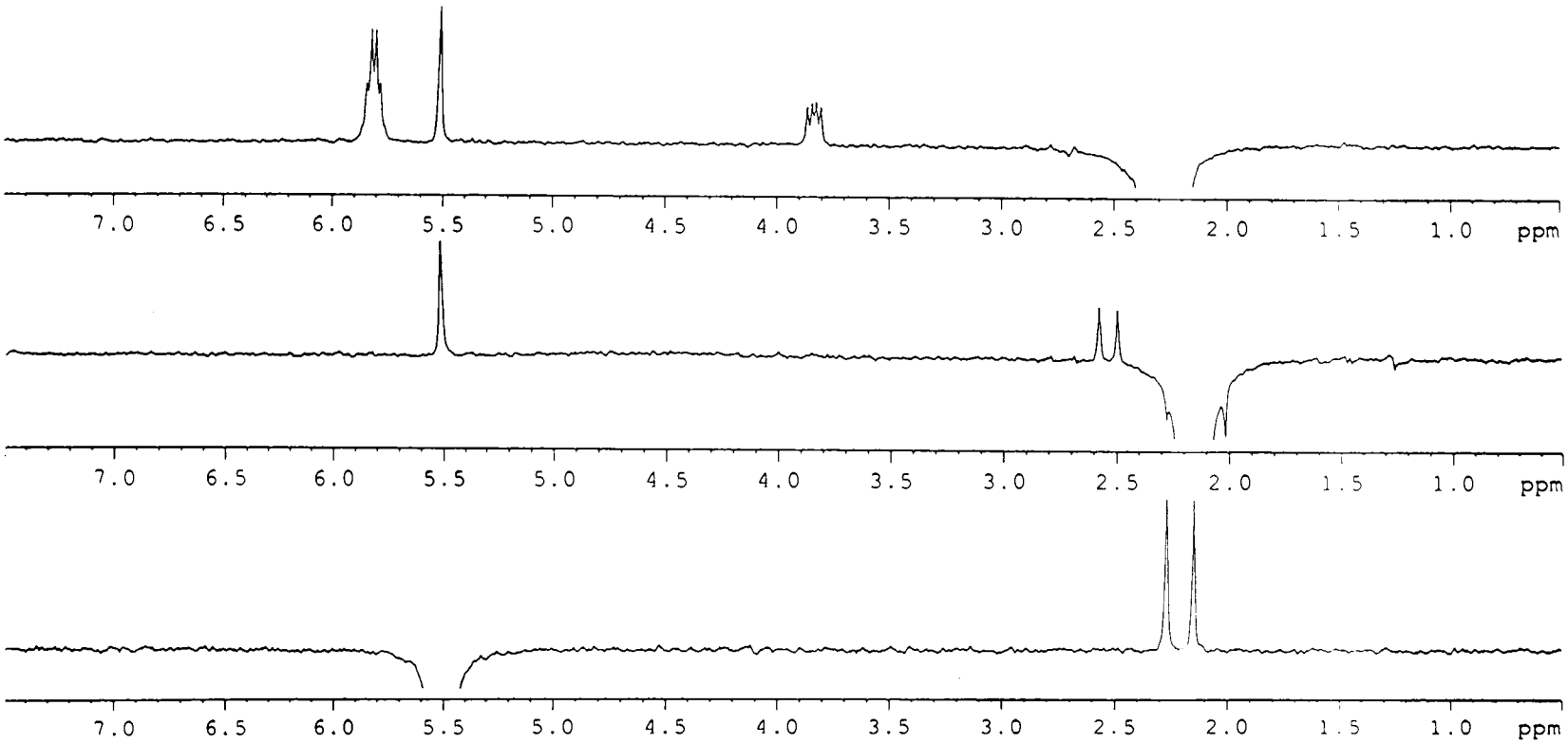

2.6 nOe Experiment with *Syn*-Isomer of Tp'Rhenium Propanemonothiodiolate

An NMR sample was first irradiated at 5.52 ppm, which was a vinylic proton signal. The correlation peaks were observed at 2.21 and 2.15 ppm, which were methyl signals on the pyrazole ring. The second irradiation was performed at 2.15 ppm, and three correlation peaks were observed at 2.59 and 2.48 ppm, which were methyl signals from methyl groups on the near by pyrazole rings, 5.52 ppm, which was the peak that was irradiated at the first time. The second irradiation indicated that the signal at 2.15 ppm belonged to methyl group, which was located on the opposite side of monothiodiolate ring due to the fact that none of the correlation between this signal and any protons on monothiodiolate ring was observed. The third irradiation was performed at 2.21 ppm, and there were three correlation peaks seen, namely, 5.52, 3.37, and 2.03 ppm. The peak at 5.52 belonged to vinylic proton on the pyrazole ring, which was irradiated at the first time. The peak at 3.37 belonged to one of the methylene protons located on monothiodiolate ring. The last peak belonged to methyl group on monothiodiolate ring. From the information above the methyl group on monothiodiolate ring should be located in a proximity to one of the pyrazole rings. Due to the fact that the correlations between one of the methyl groups on the pyrazole ring and proton signals from the monothiodiolate ring were observed, the pyrazole ring that we chose for the first irradiation should be located right above monothiodiolate ring. This isomer was assigned to be *syn*-isomer. The nOe spectrum of this isomer is shown in Figure 2.6.

Figure 2.6: nOe Spectrum of *Syn*-Isomer of Tp' Rhenium Propanemonothiodiolate

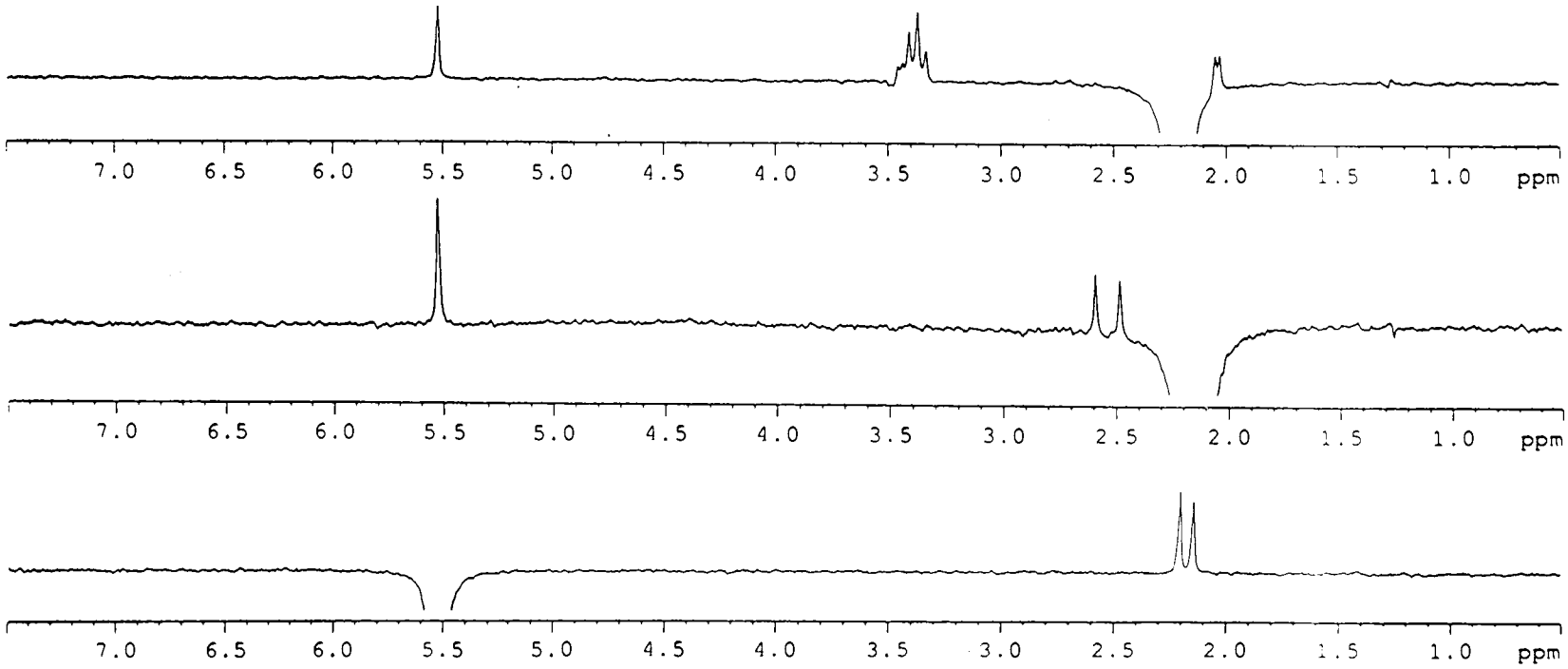

2.7 Synthesis of Phenylethane-1,2-dithiol (49)

In order to synthesize hydrido-*tris*-(3,5-dimethyl-1-pyrazolyl)borato (phenylethanedithiodiolato)(oxo)rhenium(V), phenylethanedithiol had to be synthesized first, as it is not commercially available. However, it can be synthesized via the trithiocarbonate intermediate. The synthetic plan is shown in Figure 2.7.

Figure 2.7: Synthetic Plan for the Synthesis of Phenylethanedithiol

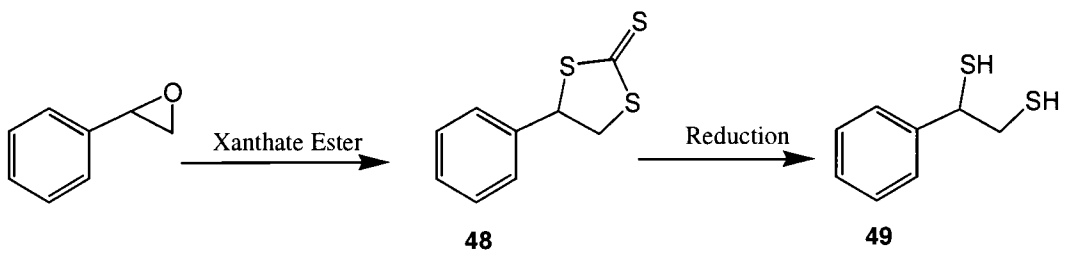

48 49

Styrene trithiocarbonate can be easily made by reaction of styrene oxide and a xanthate ion. Culvenor reported a one-pot procedure for the synthesis of styrene trithiocarbonate by using carbon disulfide and potassium hydroxide in methanol[40]. Under this condition, a xanthate ion will be generated in-situ, followed by nucleophilic attack at terminal carbon of epoxide unit of styrene oxide.

Styrene oxide, carbon disulfide, and potassium hydroxide were allowed to stir in methanol for 12 hours at room temperature. After 12 hours, a yellow solid was formed in the reaction flask due to the fact that styrene trithiocarbonate was less soluble in methanol. The reaction was evaporated to dryness by using rotary evaporator. Then, the reaction was extracted by using 2:1 toluene/water. The organic layer was then washed with saturated solution of sodium bicarbonate and water, and dried by using anhydrous magnesium sulfate. Toluene was removed by rotary evaporator. The yellow needle product was obtained in a very good yield (92.63%). This compound was characterized by ^{1}H NMR, ^{13}C NMR, IR, and mass spectrometry.

One simple approach to the dithiol should be basic hydrolysis of trithiocarbonate by alcoholic potassium hydroxide. Potassium hydroxide was allowed to stir in methanol for 15 minutes until dissolved. To this solution, styrene trithiocarbonate was then added. The reaction was heated until reflux and allowed to proceed for 12 hours. The reaction was extracted by using toluene. The organic layer was then dried over anhydrous magnesium sulfate. The solvent was removed by rotary evaporator. After solvent removal, a viscous dark brown liquid was obtained. From mass spectrometry, this compound was characterized to be the product from a dimerization process. (Figure 2.8)

Dimerization can be rationalized due to the fact that a sulfide anion is a better nucleophile than an alkoxide anion. A possible mechanism leads to the formation of this dimer is shown in Figure 2.9.

Figure 2.8: Dimerized Product from Basic Hydrolysis of Styrene Trithiocarbonate

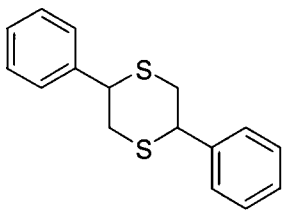

50

Figure 2.9: Mechanistic Explanation of Formation of Dimerized Product

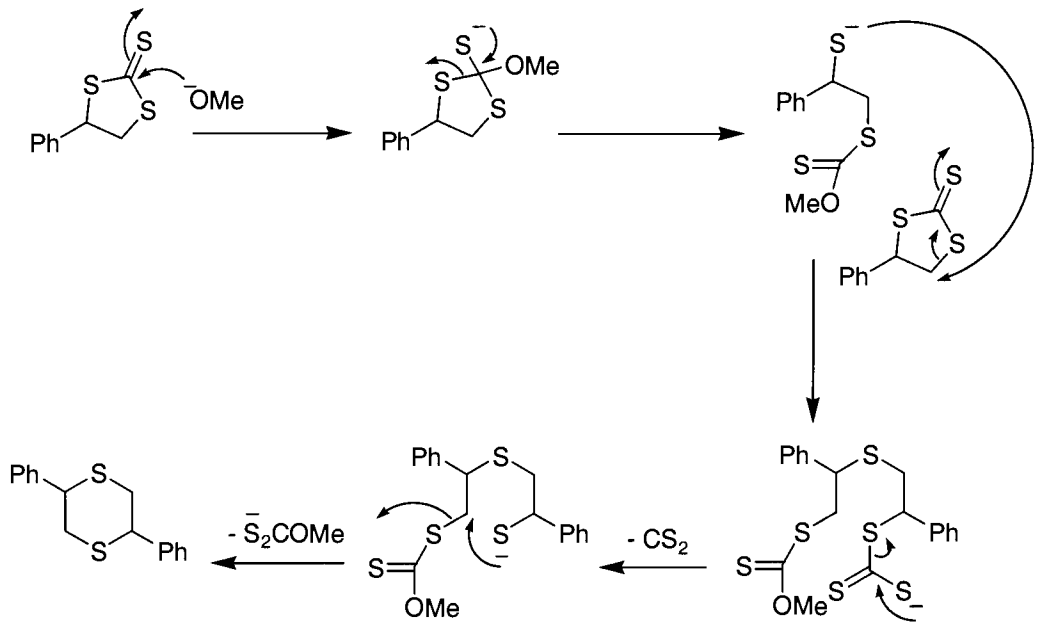

The result from basic hydrolysis led us to find a different way to convert styrene trithiocarbonate to phenylethanedithiol. According to the literature, trithiocarbonates can be reduced by lithium aluminum hydride[41]. This process leads to formation of phenylethanedithiol.

This reaction was performed under inert atmosphere of argon in order to avoid moisture from the air. 1.0 Molar lithium aluminum hydride in dry diethylether was carefully transferred into the reaction. Styrene trithiocarbonate was slowly added to the reaction as a solid. The reaction could easily be monitored by color changing from yellow to colorless. After 1 hour, the reaction was considered to be complete by TLC. Removal of solvent gave phenylethanedithiol in 87.5 %. This compound was characterized by ^{1}H NMR, ^{13}C NMR, IR, and mass spectrometry.

The splitting patterns of thiol protons, methine, and methylene protons were observed in ^{1}H NMR spectrum. The S-H stretching band at about 2550 cm^{-1} was very characteristic.

2.8 Synthesis and Characterization of Hydrido-*tris*-(3,5-dimethyl-1-pyrazolyl)borato (phenylethanedithiodiolato)(oxo)rhenium(V) (45)

Synthesis of the Tp' rhenium phenylethanedithiodiolate complex was accomplished by using the one-pot procedure described earlier. The reaction was allowed to proceed for 15 hours. Then, the reaction was filtered in order to remove ground molecular sieves. Theoretically, two different isomers should be formed,

namely, syn and anti isomers. From TLC chromatography in different solvent systems, only one broad band was observed. The product was purified by column chromatography. However, several attempts were made to separate 2 different isomers observed by ^{1}H NMR. These two isomers appeared to have the same R_f in a variety different solvent system. By careful fractionation, partial enrichment in one isomer was observed, but the separation of each pure compound was not successful. However, by using some advanced NMR techniques, the characterization of these two isomers was successfully completed.

2.9 COSY Experiment with Tp' Rhenium Phenylethanedithiodiolate

A COSY experiment was performed in order to distinguish between 6 different protons on the two dithiodiolate rings. Originally, a 1D ^{1}H NMR spectrum of this mixture was collect by using deuterated chloroform as a NMR solvent. However, there was an overlap of proton signals from the dithiodiolate ring. Consequently, the NMR solvent was change to deuterated benzene, and separation of these signals was slightly improved. In the latter NMR solvent, the coupling constants of all of 6 signals from protons on dithiodiolate ring could be extracted directly from the spectrum. The same sample in deuterated benzene was used in the COSY experiment. This COSY spectrum is shown in Figure 2.10. From the correlation peaks in this spectrum, the proton signals at 3.88, 4.62, 5.36 ppm came from one isomer. The signals at 4.30, 4.56, 4.83 ppm came from the other isomer.

The splitting patterns of all of these six signals revealed that they belonged to protons on dithiodiolate ring. All of the methyl group signals between 1.30 – 3.20 ppm did not give any useful information in this experiment due to the fact that these methyl groups were located on each pyrazole ring, and 3-bond coupling for protons was not available. There were correlation peaks in aromatic region in these compounds, which came from phenyl moiety on dithiodiolate ring. Vinylic signals at about 5.0-5.2 ppm shown very weak correlations to some of the methyl signals located around 2.1 – 3.2 ppm.

Figure 2.10: COSY Spectrum of Mixture of *Syn-* and *Anti-* Isomers of Tp'Rhenium Phenylethanedithiodiolate

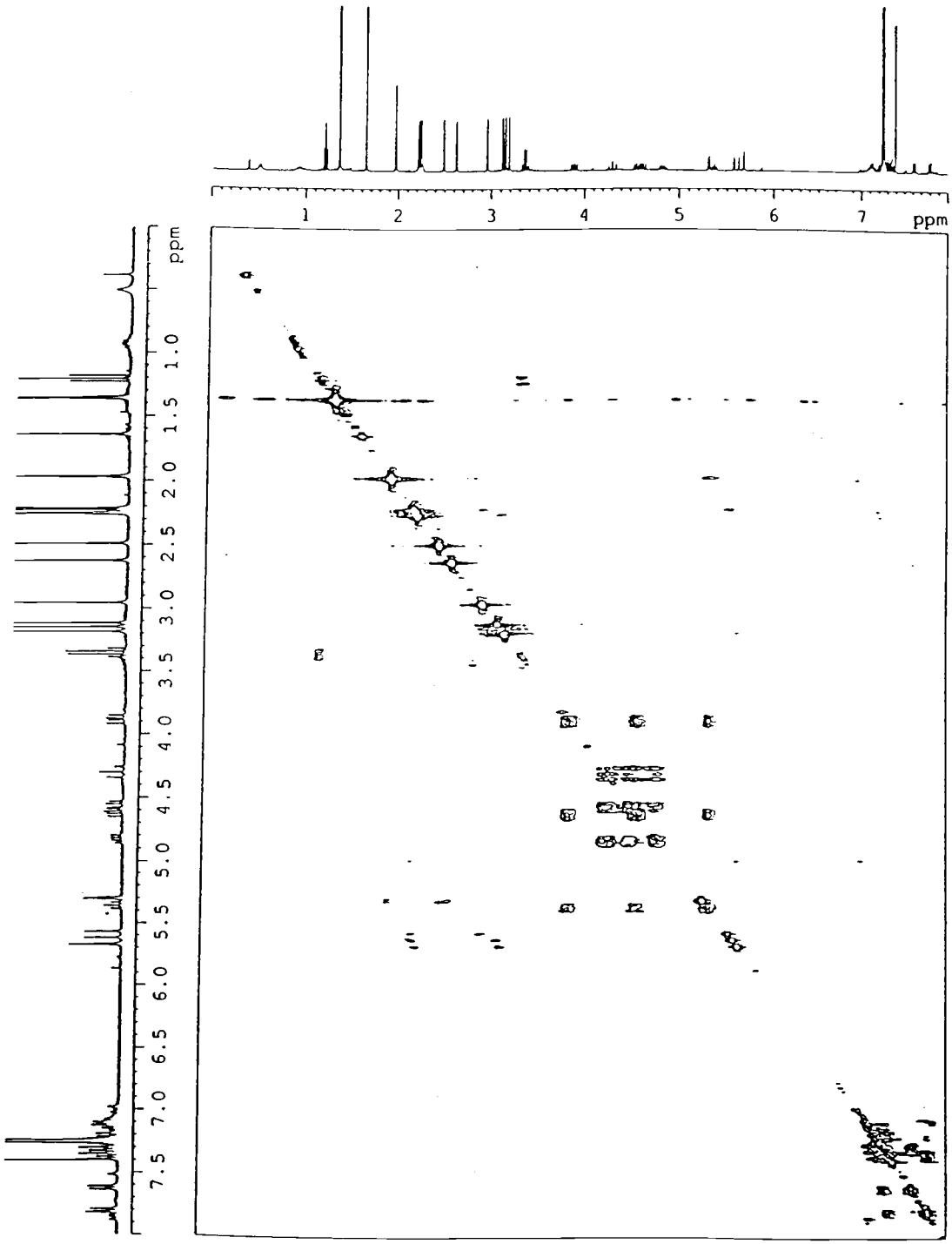

2.10 HSQC Experiment with Tp' Rhenium Phenylethanedithiodiolate

Due to the fact that there were two isomers in the mixture of Tp' rhenium phenylethanedithiolate complex, the assignment of ^{13}C NMR spectrum was a little more complicated. Namely, by direct inspection of ^{13}C NMR spectrum, some of the signals were missing. In this mixture, there should be 12 ^{13}C methyl signals coming from these two isomers. Nonetheless, from inspection of ^{13}C NMR spectrum, there were only 6 sharp peaks around 16-18 ppm, 4 broad peaks between 12.4-12.6 ppm, and the total of signals from inspection were only 10. The initial hypothesis would be that the broadening of peaks is caused by overlapping of signals. From the 1D ^{1}H NMR experiment, all 12 methyl signals in ^{1}H NMR spectrum were identified. The ratio of these two isomers in the mixture appeared to be 1:1 from integration of ^{1}H NMR signals. Thus, the correlation between ^{1}H signals and ^{13}C signals would prove the hypothesis above. If there were more than 4 proton signals correlating to 4 broad peaks around 12.4-12.6 ppm, those 4 broad peaks should be a group of signals coming from more than 4 methyl carbons in this sample, and the number of carbons can be easily determined by counting the number of protons correlating to those carbon signals. In order to solve this problem, HSQC experiment was employed. The same sample, which contained deuterated benzene as an NMR solvent, was used in this experiment. HSQC spectrum is shown in Figure 2.11, and the correlations of carbons and protons are shown in table 2.2.

Figure 2.11: HSQC Spectrum of Tp' Rhenium phenylethanedithiolate

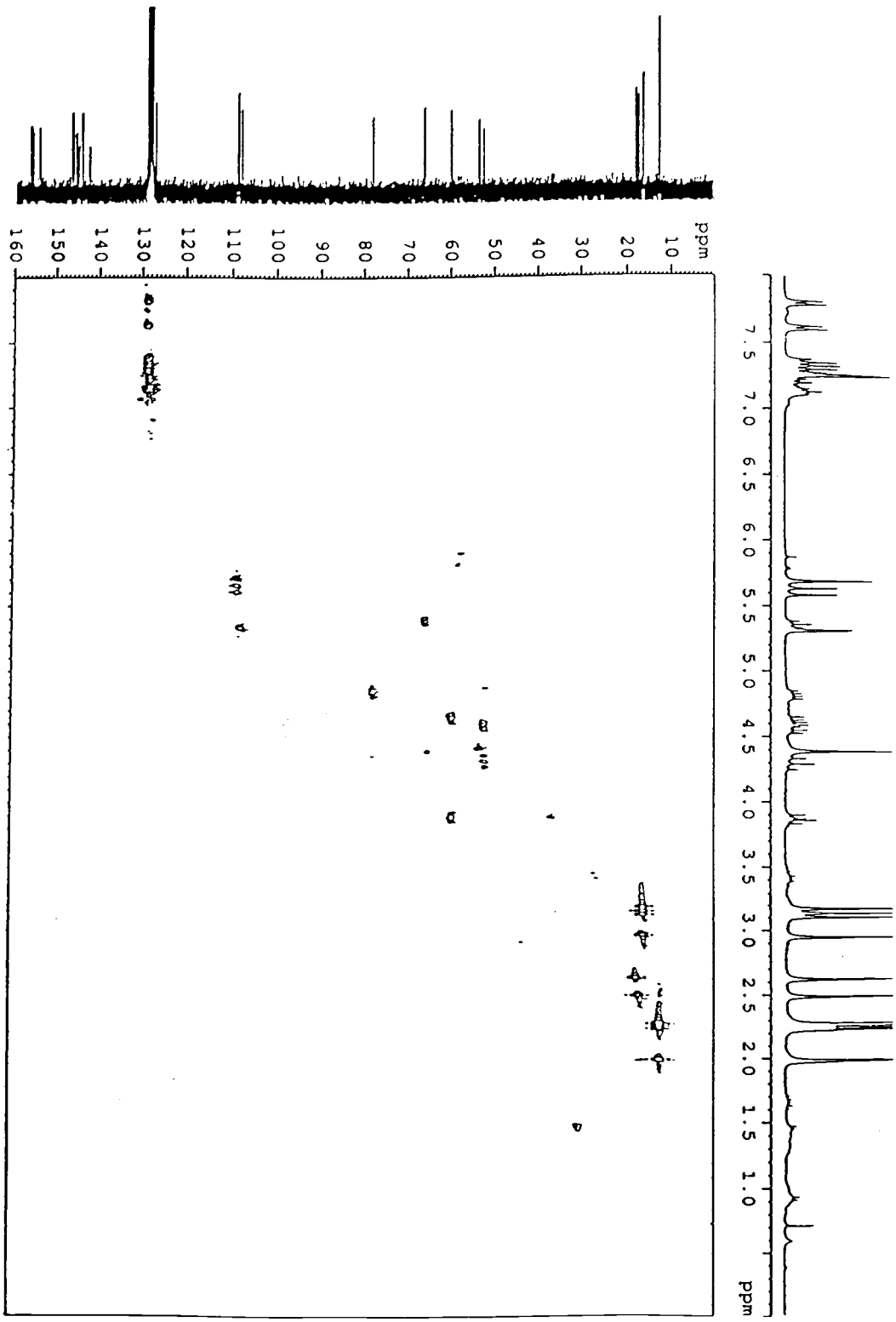

Table 2.2: NMR Results from HSQC Experiment

1H NMR shifts, ppm	Coupled carbon(s)
1.97 (6 H)	12.49 or 12.51 or
2.21 (3 H)	12.54 or 12.56
2.23 (3 H)	
2.25 (3 H)	
2.26 (3 H)	
2.49 (3 H)	17.23
2.62 (3 H)	17.82
2.95 (3 H)	16.16 or 16.18 or
3.11 (3 H)	16.21 or 16.25
3.15 (3 H)	
3.18 (3 H)	
3.88 (1 H)	59.79
4.30 (1 H)	52.43
4.56 (1 H)	52.43
4.62 (1 H)	59.79
4.83 (1 H)	77.93
5.30 (1 H)	107.98 or 108.02
5.31 (1 H)	
5.36 (1 H)	66.00
5.57 (1 H)	108.77 or 108.79 or
5.62 (1 H)	108.82 or 108.87
5.67 (2 H)	
7.1-7.4 (6 H)	127.19 or 128.74 or
7.60 (2 H)	128.81 or 128.83 or
7.79 (2 H)	128.95

From the HSQC experiment, the hypothesis about overlapping of signals was proved to be correct. Namely, there were correlations between 18 methyl protons and 4 broad carbon peaks between 12.4-12.6 ppm. The two missing carbon signals should be underneath 4 broad peaks between 12.4-12.6 ppm. A ^{13}C signal at 53.52 ppm, which correlates with a proton signal at 4.38 pm (Not shown in table 2.3 and experimental section), was assigned to be carbon of dichloromethane left from the chromatography. ^{13}C signals at 52.43 and 59.79 ppm were assigned to be methylene carbons on the dithiodiolate ring of one isomer, and ^{13}C signals at 66.00 and 77.93 ppm were assigned to be methine carbons on dithiodiolate ring of the second isomer. There were correlations between aromatic protons around 7.00-7.90 ppm, which belonged to two phenyl rings in each isomer, and sp^2 carbon around 127-130 ppm. However, there was one peak missing for an aromatic carbon. Presumably, this peak might be under carbon peaks from deuterated benzene. This statement cannot be confirmed by this experiment due to the limitation of resolution. Information from COSY and HSQC experiments was sufficient to distinguish between six different protons on dithiodiolate ring. Namely, three of them should come from *syn*-isomer, and the rest would come from *anti*-isomer. Nevertheless, in order to characterize which three come from which isomer, nOe experiment should be performed.

2.11 nOe Experiments with Tp' Rhenium Phenylethanedithiodiolate

For nOe experiments, not only methylene protons and methine protons were characterized, but some of methyl signals were also assigned for each isomer. Several sequential irradiations were done, but only the experiments giving useful information for identification of each isomer will be discussed.

Sequential irradiation experiments were performed. An NMR sample was irradiated at 5.32 ppm, which was previously assigned to be the vinylic signal from a pyrazole ring of the Tp' ligand. The correlation peaks appeared at 1.99, 2.49, and 2.63 ppm. Due to the integration of methyl signal at 1.99 ppm, there should be 2 methyl signals at this position. Consequently, there were 4 methyl groups correlated to vinylic signals at 5.32 ppm. This result was consistent with the number of vinylic protons at 5.32 ppm, which the integration shown to be 2 protons. Indeed, one vinylic proton should correlate to only 2 methyl groups located on the same pyrazole ring.

The second irradiation was done at 2.63 ppm. The correlation peaks were obtained at 7.80, which was one signal from a phenyl group, 5.32, which was the peak that first irradiated, and 4.30 ppm, which was one of the protons on dithiodiolate ring. This proton was assigned to be one of the methylene protons by the HSQC experiment. The pyrazole ring that we chose for the first irradiation should be located right above the dithiodiolate ring because the correlation between methyl signal at 2.62 ppm and one of the methylene protons at 4.30 was seen. Due to the fact that the correlation between phenyl signal and methyl signal on the

pyrazole ring was seen, these signals were assigned to be the ones originated from *syn*-isomer. From COSY, nOe, and HSQC experiments, all methylene and methine signals were completely assigned. Namely, methylene signals at 4.30, 4.56 ppm, methine signal at 4.83 ppm, and the methyl signal at 2.62 ppm belonged to the syn isomer. Methylene signals at 3.88, 4.62 ppm, and methine signal at 5.36 ppm belonged to the anti isomer. The nOe spectrum of Tp' rhenium phenylethanedithiolate is shown in figure 2.12.

Figure 2.12: nOe Spectrum of Tp' Rhenium Phenylethanedithiodiolate

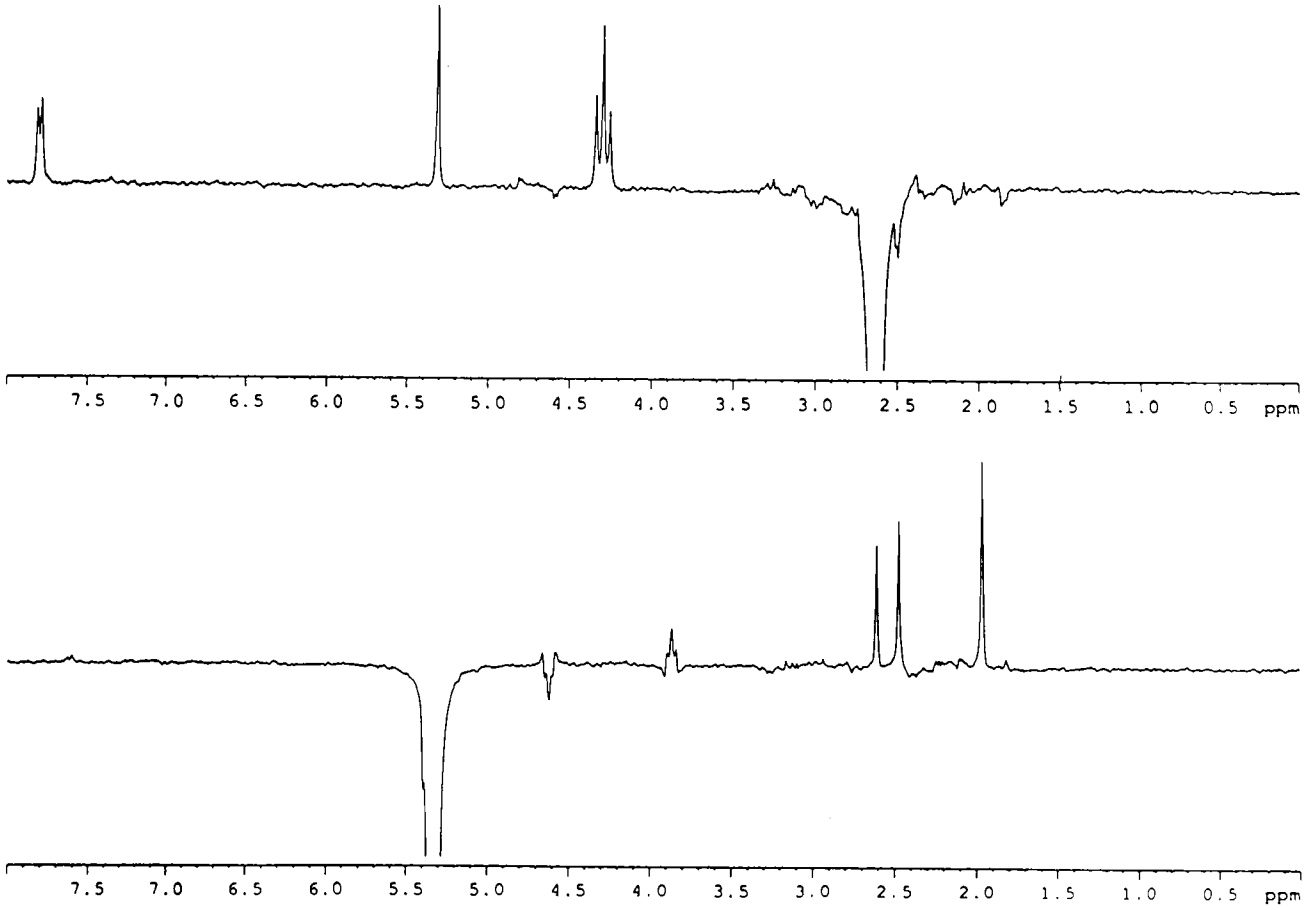

2.12 Determination of Dihedral Angles of the Diolate Ring of Tp' Rhenium Dithiodiolate And Monothiodiolate Complexes in Solution

From the Karplus equation, the coupling constants of protons in an alkane or alkene and the dihedral angle between them are mathematically related (Figure 2.13)[42].

Figure 2.13: Karplus Equation

$$J = A + B\cos(\Phi) + C\cos(2\Phi)$$

Where: A, B, and C = empirical constants

Φ = dihedral angle (H-C-C-H)

There are some modifications of the Karplus equation in order to make it applicable to the different systems with the different atoms. In this experiment, the Karplus-type relationship corrected for the electronegativity of substitiuents modified by Pachler[43] was used (Figure 2.14).

In solution, the dithiodiolate or monothiodiolate rings will be flexible. Therefore, the observed coupling constants will be an average values caused by two different structures shown in Figure 2.15.

Figure 2.14: Karplus Equation Modified by Pachler

$$J_x = A_x + B_x\cos\Phi + C_x\cos 2\Phi + D_x\sin\Phi + E_x\sin 2\Phi$$

Where: $A_x \ldots E_x$ = empirical parameters derived from a least-squares treatment of a large number of experimental coupling constants

Φ = dihedral angle (H-C-C-H)

The calculations were performed by using a javascript-based program for calculating coupling constants from dihedral angles, which was available on the web[44]. All the coupling constants of Tp' rhenium ethanedithiodiolate were listed in Table 2.3.

Table 2.3: List of Coupling Constants of Tp' Rhenium Ethanedithiodiolate

	$J^{AB} = J^{A'B'}$ (Hz)	$J^{AA'}$ (Hz)	$J^{AB'}$ (Hz)	$J^{A'B}$ (Hz)	$J^{BB'}$ (Hz)
Ethanedithiodiolate	-12	5.95	7.54	7.42	6.87

Figure 2.15: Two Conformations in Solution of Tp' Rhenium Ethanedithiodiolate

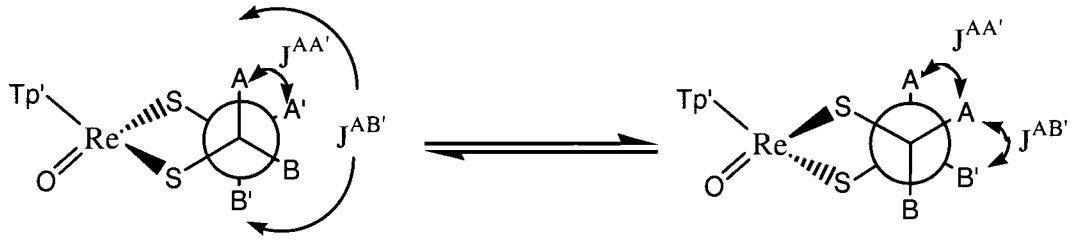

From Figure 2.15, the dihedral angle between H_A and $H_{A'}$ protons would be similar in these two structures. However, the dihedral angle between H_A and $H_{B'}$ should be an average of those two structures. From the Karplus calculator, the average of the angle from this coupling constant was about 78°. For tetrahedral carbon, angle between H_A and H_B should be 120°. Consequently, this assumption led to the dihedral angle between H_A and $H_{A'}$ of about 42°. By substituting $J^{AA'}$ into Karplus calculator, the dihedral angle was about 34°. By averaging 42° and 34°, the average H-C-C-H dihedral angle of this system would be 38°. In this calculation, Br atoms were used instead of sulfur in order to account for the effect of electronegativity on dihedral angle. The same calculation was done with Tp' rhenium ethanemonothiodiolate complex, and the average value for H-C-C-H dihedral angle was 41°. For other compounds, the calculated dihedral angles are shown in Table 2.4.

Table 2.4: Vicinal Coupling Constants and Calculated Average H-C-C-H Dihedral Angles

Compound	J, Hz	Dihedral Angle
Syn ethane-1-thio-2-methyl-1, 2-diolate	6.3	25.8
Anti ethane-1-thio-2-methyl-1, 2-diolate	6.6	23.7
Syn phenylethanedithiolate	6.3	32.5
Anti phenylethanedithiolate	7.2	26.1

From Table 2.4, the dihedral angles shown here for dithiodiolate and monothiodiolate complexes are still smaller than that for diolate complexes[45]. This observation indicates the effect of electronegativity of substiuents in this case sulfur atom(s). The small dihedral angle for the phenylethanedithiolate may arise from the steric interaction with the pyrazole methyl group. In conclusion, substitution of oxygen by sulfur atom(s) in diolate complex leads to a smaller H-C-C-H dihedral angle, that is, flatter conformation of the diolate ring. In case of Tp' rhenium ethanedithiodiolate complex, conformation in solution is different from the one in solid state. Namely, the dihedral angle in solution is about 38^{o},which is pretty large, compare to 12^{o} in solid state (see below).

2.13 Recrystallization and X-ray Crystal Structure of Tp' Rhenium Dithiodiolates

The dark yellow solid Tp' rhenium dithiodiolates can be recrystallized in a mixed system of acetonitrile and water. The details for recrystallization process are fully explained in experimental chapter. The crystals obtained from this process were then used in X-ray crystal structure analysis. The ORTEP from crystallographic analysis is shown in Figure 2.16.

Figure 2.16: ORTEP from the X-ray Crystallographic Analysis of Tp' Rhenium Dithiodiolate

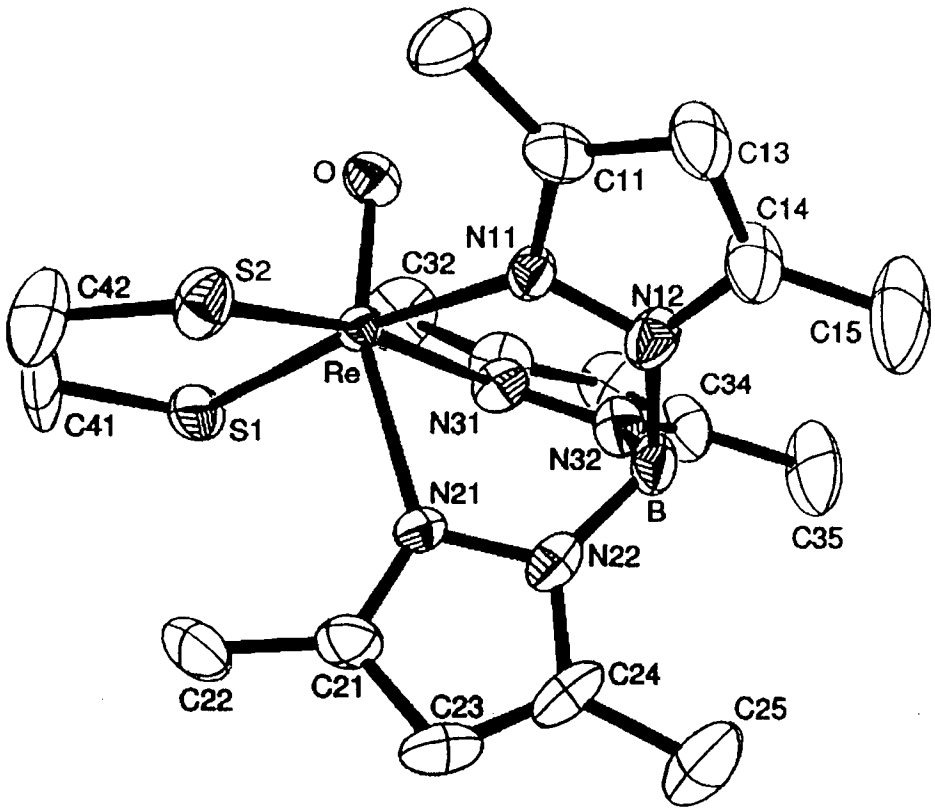

Some of the parameters from X-ray crystallographic analysis are shown in Table 2.5. From crystallographic data, the dihedral angle in dithiodiolate ring (C-S-S-C) is only 12.1 degree.

Table 2.5: Selected Bond Lengths And Bond Angles of Tp' Rhenium Ethanedithiodiolate

	Distances (Angstrom)
Re-S_1	2.286
Re-S_2	2.273
Re-O	1.663
Re-N_{21}	2.275
Re-N_{31}	2.130
Re-N_{11}	2.183
	Bond Angles (Degree)
ReS_2C_{42}	106.7
ReS_1C_{41}	107.6
S_1CCS_2	12.1

From Table 2.5, Re-O is short due to the fact that it is formally a triple bond. This compound shows an unusually flat conformation of dithiodiolate ring in solid state from the small dihedral (S-C-C-S) angle. In conclusion, solid state structure of this compound is imposed by crystal packing forces, and the barrier to ring flip or other distortion is very low.

2.14 Attempted Cycloreversion of Tp' Rhenium Dithiodiolate and Monothiodiolate Complexes

Cycloreversion reactions for Tp' rhenium dithiodiolates and monothiodiolates were attempted in deuterated benzene, and monitored by ^1H NMR spectroscopy. 1,4-di-*tert*-butylbenzene was added as an internal integration standard. All of these compounds appeared to be thermally stable at the temperature up to 120 °C for 7 days. Namely, none of the alkene signal was observed, and integration of the dithiodiolate or monothiodiolate versus 1,4-di-*tert*-butylbenzene had changed by less than 3%. Herrmann reported that Cp* rhenium ethanedithiodiolate completely decomposed in 30 minutes at 200 °C. In the case of Tp' rhenium dithiodiolates and monothiodiolates, if these compounds had underwent the cycloreversion reaction at a similar rate, more than half of the complexes would have been converted to alkenes, and the integration should significantly be changed.

2.15 Energetics of Alkene Addition to ReS_4^-

This observation led to the consideration of ReS_4^- work reported by Rauchfuss[46]. Rauchfuss reported that, experimentally, cycloaddition of alkenes to ReS_4^- appeared to be thermodynamically favorable process. Indeed, reaction of the initial alkene binding adduct and H_2S result in a more stable adduct. The qualitative

reaction coordinate was illustrated in his work. This led us to consider the quantitative energetics of some of the specific reactions in this process.

The calculations were performed by using DFT (Density Functional Theory), and an effective core potential basis set, which simplifies the computation. All of the structures were first optimized by using molecular mechanics calculation. Then, the DFT calculations were performed by using LACVP** basis set with B3LYP functionals. The calculations were done with the structures shown in Figure 2.17, and heat of reactions of coupling of H_2S and ethylene additions to ReS_4^- are shown in Figure 2.18.

Figure 2.17: Structures Used in DFT Calculation (LACVP** with B3LYP Functionals)

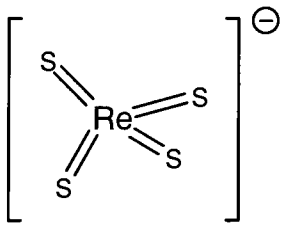

31

9

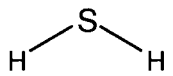

51

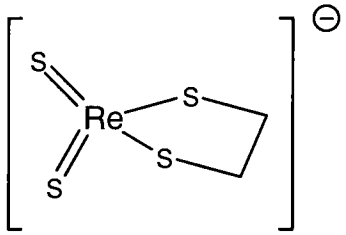

33

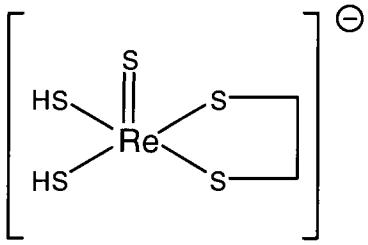

34

Table 2.6: The Energies of Minimized Structures Shown in Figure 2.17

	Hatree	kcal/mol
Ethylene	-78.59197493	-49316.46427
ReS_4^-	-1671.924128	-1049132.39
$ReS_4C_2H_4^-$	-1750.540594	-1098464.222
H_2S	-399.388764	-250616.4528
$ReS_5C_2H_6^-$	-2150.106478	-1349191.815

Figure 2.18: Heat of Reaction of Coupling of H_2S and Ethylene Additions to ReS_4^-

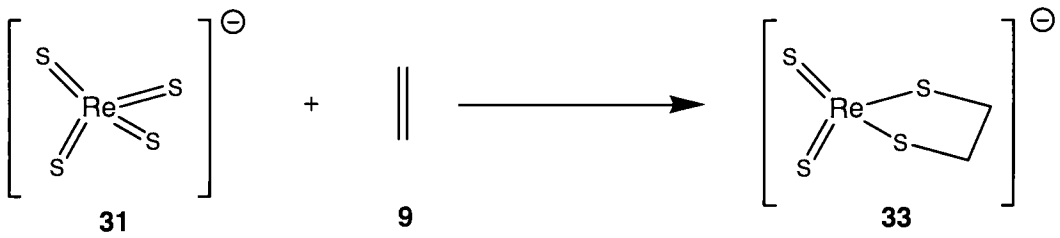

31 9 33

Heat of reaction = -0.02449 Hatrees (-15.4 kcal/mol)

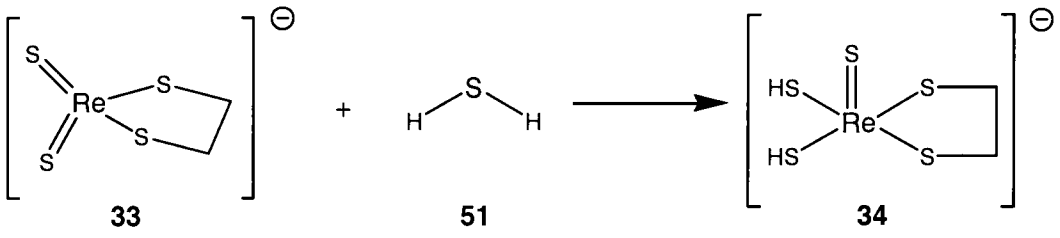

33 51 34

Heat of reaction = -0.17712 Hatrees (-111.1 kcal/mol)

The results from calculations are consistent with Rauchfuss's work. Alkene addition to ReS_4^- is an exothermic process. In case of norbornene, the ΔH^o_{rxn} was calculated to be –12.67 kcal/mol. From Rauchfuss's work, the kinetic barrier between ReS_4^- and alkene adduct appears to be low, and the system can be driven to the formation of alkene adduct by trapping with a Lewis base, which is thiol. Indeed, from this DFT calculation, reaction of alkene adduct and H_2S, which is a second reaction, appeared to be even more exothermic. From this calculations, The H_2S adduct is more stable than alkene adduct of ReS_4^-. This observation is consistent with the experimental data reported by Rauchfuss[47]. The stabilization aroused from adding H_2S across Re=S bond can be explained by "Spectator sulfido effect." This concept was originated from "spectator oxo effect" aroused from quantum calculations by Rappe' and Goddard in 1982[48] showing that the formation of one strongly bonded terminal M=E (E=O, NR) could be a driving force for binding reagents to $M(=E)(=E')X_2$. In 1998, Coucouvanis[49] applied an analogous spectator sulfido effect to explain the reactivity of tetrahedral $Mo(=S)_2X_2$ species. In conclusion, this experiment provided the useful information concerning stability of dithiolate adducts.

The DFT calculations of cycloreversion reaction of Tp' rhenium dithiodiolate and monothiodiolate were reported (Table 2.7)[50]. Substitution of sulfur for oxygen atom(s) stabilized the monothiodiolate or dithiodiolate complexes by a significant amount of energy. For calculated energies of cycloreversion reaction, substitution of each sulfur atom raises the calculated ΔE_{rxn} by about 10

kcal/mol. This result is consistent with the experimental observation of the reactivity of these compounds. Namely, these complexes fail to cyclorevert at temperature up to 120 °C for 7 days. This is because of the thermodynamic stability of monothiodiolate and dithiodiolate complexes.

For the Tp' rhenium ethanedithiodiolate complex, which X-ray crystal structure was analyzed in our previous experiment, the comparison between X-ray crystal structure and optimized structure obtained from DFT calculation revealed differences geometry in solid state and solution. Some parameters are shown in Table 2.8. The most significant feature will be the difference in dihedral angle (S-C-C-S) between these two different experiments. In X-ray crystal structure, the dihedral angle appear to be 12° which is a lot smaller than that in solution which is about 43°. However, as this angle appears to be a consequence of crystal packing, the calculated structure appears to be consistent with the solution structure.

Further evidence of thermodynamic stability of these compounds can be seen from mass spectrometry. None of these compounds show a $(M\text{-alkene})^+$ signal, as can be observed in the case of Tp' rhenium diolate complexes. Instead of $(M\text{-alkene})^+$ signal, $(M\text{-pyrazole-alkene})^+$ signal was observed. These observations suggest that fragmentation of pyrazole ligand from the parent ion is more favorable and that the loss of the alkene can occur only after the fragmentation of pyrazole ligand.

Table 2.7: DFT Calculations of Cycloreversion Reaction of Tp' Rhenium Dithiodiolate And Monothiodiolate Complexes

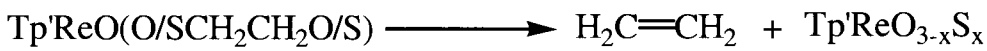

X	Energies (Hartree)			ΔE (Hartree)	ΔE (kcal/mol)
0	-1321.8216	-78.5938 (6-31G**)	-1243.1956	+0.0322	+20.2
1	-1644.7989		-1566.1558	+0.0493	+30.9
2	-1967.7795		-1889.1185	+0.0672	+42.2

Note : B3LYP Methodology with LACVP** Basis set

In conclusion, substitution of oxygen atom(s) by sulfur atom(s) in diolate ring not only increases the thermodynamic stability of the complexes, but also decreases the dihedral angle between two methylene groups in diolate ring.

Table 2.8: Comparison of Parameters from X-Ray Crystal Structure and Optimized Structure by DFT Calculation of Tp' Rhenium Ethanedithiodiolate Complex

	X-Ray Crystal Structure	DFT Calculation
	Distances (Angstrom)	Distances (Angstrom)
$Re\text{-}S_1$	2.286	2.3362
$Re\text{-}S_2$	2.273	2.3354
Re-O	1.663	1.6950
$Re\text{-}N_{21}$	2.275	2.3720
$Re\text{-}N_{31}$	2.130	2.2055
$Re\text{-}N_{11}$	2.183	2.2063
	Bond Angles (Degree)	Bond Angles (Degree)
ReS_2C_{42}	106.7	106.9578
ReS_1C_{41}	107.6	101.9585
S_1CCS_2	12.0	43.0590

2.16 Reaction of a Rhenium Dioxo Complex and Ethylene sulfide

According to previous work in the Gable group concerning deoxygenation of epoxide by using Tp' rhenium (V) oxides shown that epoxides react with reduced rhenium species and net O-atom transfer from epoxides to a phosphorus reductant was completed at 75-105 °C[51]. From this observation, the deoxygenation may proceed via 2 different processes shown in Figure 2.19.

Figure 2.19: Two Proposed Pathways for Deoxygenation

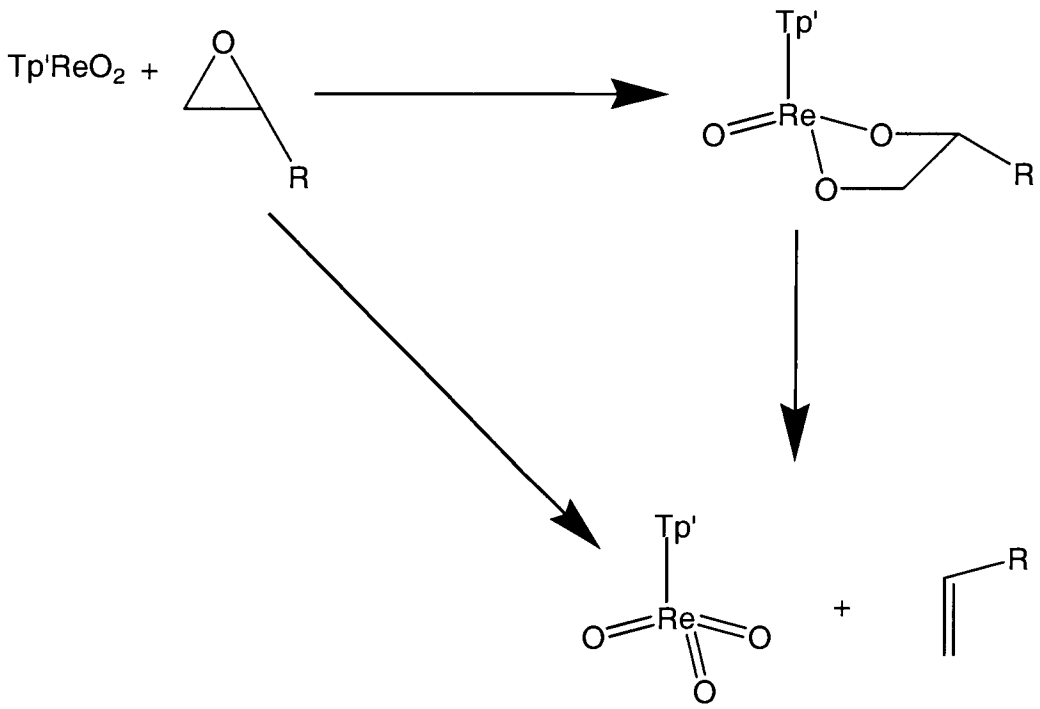

From Figure 2.19, it is interesting to see whether episulfides, which are sulfur analogs of epoxides, exhibit the same reactivity. From previous experiments concerning stability of monothio and dithiodiolate complexes toward the cycloreversion reaction and stabilization by substituting sulfur for oxygen atom(s) in DFT calculations, the ring expansion of coordinated ethylene sulfide should be observed when Tp' rhenium dioxo complex reacts with ethylene sulfide. In order to test this hypothesis, the reactions of rhenium dioxo complex and ethylene sulfide were performed both with and without acid catalysis. Unexpectedly, the Tp' rhenium ethanedithiodiolate complex was formed in about 30% yield under both conditions. From this result, there should be multiple processes involved leading to this type of product. Based on stoichiometry, sulfur atoms have to incorporate into the structure of the product in two steps. A proposed mechanism for this transformation is shown in Figure 2.20. The first step will be the coordination of ethylene sulfide to Tp' rhenium dioxo complex followed by extrusion of alkene. The product from the first two steps will be Tp' rhenium dioxo monosulfido complex. The next step will be selective reduction of Tp' rhenium dioxo monosulfido complex by O atom transfer rather than S atom transfer to triphenylphosphine. The resulting Tp' rhenium monooxo monosulfido complex can then react with another ethylene sulfide molecule, resulting in a coordinated ethylene sulfide species. The last step will be ring expansion giving Tp' rhenium ethanedithiodiolate complex. In the last step, we propose that the ring expansion

process is faster than direct alkene extrusion. The driving force for ring expansion process in the last step of this mechanism might be the thermodynamic stability of Tp' rhenium dithiodiolate product.

Figure 2.20: Proposed Mechanism for Reaction of Rhenium Dioxo Complex and Ethylene Sulfide

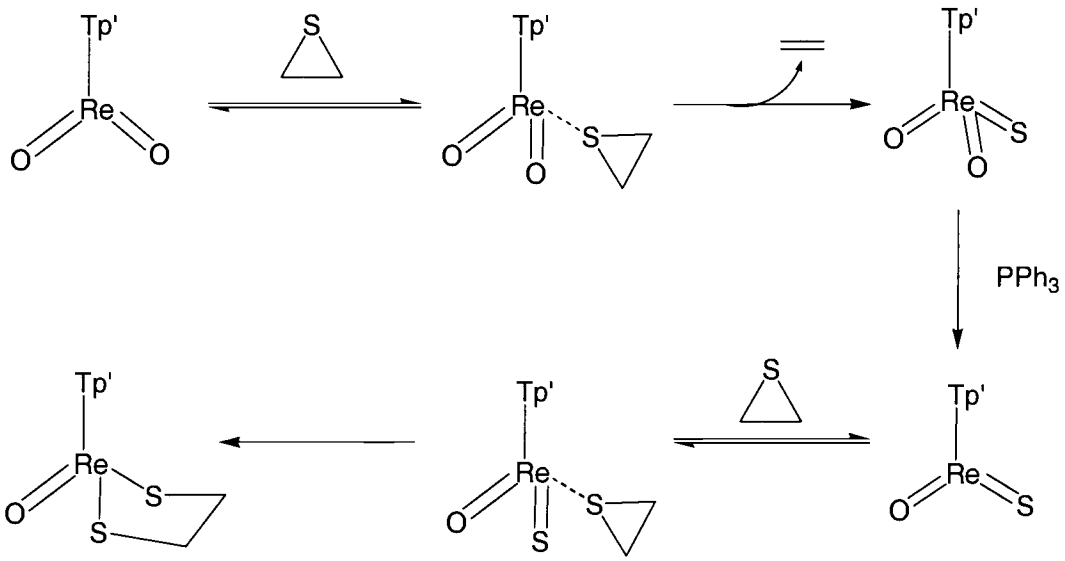

It is conceivable to think of Tp' rhenium monothiodiolate complex, which may be formed from the ring expansion process, as an intermediate of this process. (Figure 2.21)

Figure 2.21: Formation of Tp' Rhenium Monothiodiolate Complex

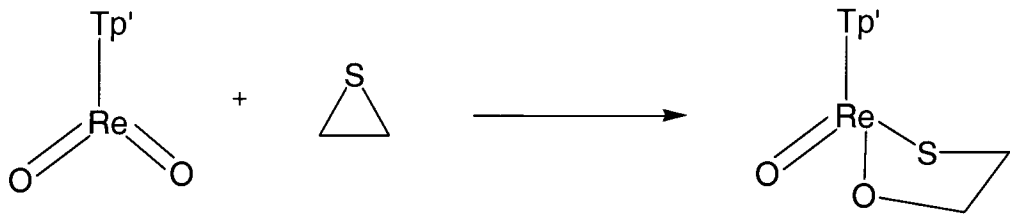

In the second step shown in Figure 2.20, there may be 2 competing steps going on, namely, the ring expansion giving the mothiodiolate complex and direct extrusion of alkene, which was shown here. In order to test whether the monothiodiolate complex is an intermediate in this process, this experiment was rerun in the presence of a small amount of Tp' rhenium monothiodiolate complex. After 15 hours, the crude product of this reaction was analyzed by ^{1}H NMR spectroscopy. The signals of Tp' rhenium monothiodiolate were still easily detectable from the spectrum. The quantitative analysis of this species in the mixture was unnecessary due to the fact that the compound must be consumed rapidly if it was really an intermediate for this reaction. Indeed, this compound was added into the reaction in very low amount, consequently, it should be totally consumed during the course of reaction if it were an intermediate. This observation suggested that the ring expansion of coordinated episulfide complex formed in the first step of the mechanism should be slower than the direct extrusion of alkene from this species. This conclusion may conflict with the explanation of the last step

in the mechanism proposed above. Namely, in the last step, the coordinated epoxide species should undergo direct alkene extrusion in order to get the Tp' rhenium ethanedithiodiolate product. However, it is important to note that the thermodynamic barrier of these two steps should be somewhat different due to the fact that Tp' rhenium ethanedithiodiolate complex is more stable than Tp' rhenium ethanemonothiodiolate complex by about 10 kcal/mol from DFT calculation[50]. However, the energies of other species such as all of the coordinated episulfides have never been calculated.

2.17 Reaction of Rhenium Dioxo Complex and Cyclohexene Sulfide

From the result of reaction of rhenium dioxo complex and ethylene sulfide, the same type of chemistry would be expected for cyclohexene sulfide. The reaction was performed both with and without acid catalysis, and both conditions gave the same result. After 15 hours, the reaction mixture turned dark green, and the crude product was chromatographed using 1:1 dichloromethane/hexane. From TLC experiment, there were 3 different spots of green complexes. However, further purification of the product was unsuccessful. Only a mixture of 2 compounds could be isolated from this reaction. The ^{1}H NMR of this mixture shown complicated signals around 1.00-3.50 ppm, which presumably belonged to methylene protons in cyclohexane ring. The overall ^{1}H NMR spectrum of this mixture was different from the spectrum of dithidiolate complex. For example, the methylene protons on the

dithiodiolate ring were not observed, and vinylic proton signals seemed to belong to C_1 symmetry species. Integration of each signal didn't reflect the reasonable ratio of protons because the sample was not a pure compound. In the infrared spectrum, the Re=O stretching in Tp' rhenium dithiodiolate complex at 940 cm^{-1} was not seen in this mixture. Mass spectrometry shown a significant peak at m/z = 678.2, which might arise from one Tp' rhenium monooxo complex, one cyclohexene sulfide molecule, and two sulfur atoms. However, based on all the information we have, the full characterization of these compounds was unsuccessful.

Chapter 3. Experimental

3.1 General Techniques

The manipulations of air-sensitive compounds in all experiments are described in the literature[52]. All reactions were performed under argon using a double-manifold Schlenk line. All chemicals were used as received from Aldrich. THF was completely dried by distillation from sodium/benzophenone. Column chromatography was performed by using silica gel (Scientific, Catalog Number: 162544, Particle Size: 32-63, Lot Number: 22521). The infrared spectrometer used was a Nicolet Magna-IR 560 Spectrometer. All NMR spectra were collected on a Bruker DP300 NMR Spectrometer. The field strength of the spectrometer was 300.13 MHz for ^{1}H, 75.04 MHz for ^{13}C. All chemical shifts were referenced to residual proton or carbon in solvent and expressed in ppm downfield from tetramethylsilane. Coupling constants for AA'BB' system were determined by using spectrum matching methodology performed by Nuts program[53].

3.2 Synthesis and Characterization of Potassium Hydrido-*tris*-(3,5-dimethyl-1-pyrazolyl)borate (52)

The potassium Tp' salt was synthesized according to the previous report[54]. To 5.00 g of 3,5-dimethylpyrazole, KBH_4 (0.70 g, 0.01 mol) was added. The solution was heated to 170 ^{o}C. After 30 minutes, hydrogen gas evolution stopped. The solution

was then heated to 190-200 °C for 20 minutes. The white solid product (3.27 g, 9.72 mmol, 74.8%) was washed with toluene and hexane. IR (KBr pellet): 3120.56 (m), 2925.13 (s), 2861.88 (s), 2811.65 (m), 2729.72 (w), 2539.62 (s), 2354.27 (m), 2311.12 (w), 2218.10 (m), 1535.32 (s), 1482.94 (s), 1416.14 (s), 1347.37 (s), 1189.84 (s), 1158.01 (s), 1071.49 (s), 1025.44 (s), 976.66 (s), 814.86 (s), 769.13 (s), 724.17 (S), 678.74 (s) cm^{-1}.

3.3 Synthesis and Characterization of Hydrido-*tris*-(3,5-dimethyl-1-pyrazolyl)borato(trioxo)rhenium(VII) (28)

Synthesis of Tp'ReO_3 was achieved by using the methodology initially reported by Herrmann[55], and modified by Mayer[56]. To a solution of Re_2O_7 (1.45 g, 2.98 mmol) in CH_3CN, trifluoroacetic anhydride (0.44 ml, 2.98 mmol) was added. A clear pale green solution was seen after stirring for 10 minutes. KTp' (2 g, 5.95 mmol) was then added. The solution was stirred for 1 hr. The pale brown solid product (1.90 g, 3.56 mmol, 83.34%) was collected and washed with water and then hexane. ^1H NMR ($CDCl_3$): δ 2.34 (s, 9H), 2.83 (s, 9H), 5.89 (s, 3H) ppm. IR (KBr pellet): 314.35 (w), 2928.83 (w), 2546.63 (w), 1545.27 (s), 1451.19 (S), 1416.39 (m), 1389.88 (w), 1370.34 (s), 1213.29 (s), 1188.89 (m), 1069.71 (s), 1048.60 (m), 990.64 (w), 938.06 (m), 906.80 (S), 864.89 (m), 814.19 (m), 786.73 (w), 687.06 (w), 646.47 (w) cm^{-1}.

3.4 General Procedure for the Thiodiolate and Dithiodiolate Synthesis

The syntheses of thiodiolate and dithiodiolate were performed according to the previous report on the synthesis of Tp' rhenium diolates from the Gable group[57]. This methodology worked well with the system containing one or two sulfur atoms. However, the stoichiometric ratio of all of the starting materials was also optimized in order to get the best yield. Tp'ReO_3 (100 mg, 0.188 mmol), triphenylphosphine (60.89 mg, 0.236 mmol), ethanedithiol (52.72 mg, 0.561 mmol), *p*-toluenesulfonic acid (2.0 mg, 0.012 mmol), ground molecular sieves (0.5 g) were allowed to stir at room temperature for at least 15 h in 25 mL of THF. The solution was filtered, and the solvent was removed in vacuo. The product was purified by chromatography on silica gel; elution with 1:1 dichloromethane/hexane and removal of solvent was used to isolate the product.

3.5 Synthesis and Characterization of Hydrido-*tris*-(3,5-dimethyl-1-pyrazolyl)borato(ethane-1,2-dithiodiolato)(oxo)rhenium(V) (44)

From 100 mg Tp'ReO_3, 60.89 mg of triphenylphosphine, and 52.72 mg (0.561 mmol) ethanedithiol, 97 mg (0.16 mmol, 87.2%) dark brown product was obtained. ^{1}H NMR ($CDCl_3$): δ 2.14 (s, 3H), 2.17 (s, 3H), 2.54 (s, 6H), 2.89 (s, 6H), 3.5918 (AA'BB', 1H, J = 12.16, 5.95, 7.54 Hz), 3.5924 (AA'BB', 1H, J = 11.9611, 7.42, 7.54 Hz), 4.0987 (AA'BB', 1H, J = 12.16, 6.87, 7.42 Hz), 4.0994 (AA'BB', 1H, J = 11.96, 6.87, 7.54 Hz), 5.50 (s, 1H), 6.04 (s, 2H) ppm. ^{13}C NMR ($CDCl_3$): 12.97,

16.17, 17.23, 51.09, 108.09, 108.94, 143.13, 145.93, 153.94, 156.03 ppm. IR (KBr pellet): 3121.01 (w), 2955.24 (w), 2923.94 (m), 2532.41 (m), 2360.66 (w), 1545.54 (s), 1491.91 (w), 1448.92 (s), 1415.76 (s), 1380.88 (m), 1365.43 (s), 1210.98 (s), 1183.05 (m), 1065.02 (s), 1044.48 (m), 984.40 (w), 941.53 (s), 877.38 (w), 861.07 (m), 814.09 (s), 795.66 (m), 690.27 (m), 644.66 (s) cm^{-1}. MS (FAB): 592 (M^+)

3.6 Synthesis and Characterization of Hydrido-*tris*-(3,5-dimethyl-1-pyrazolyl)borato(ethane-1,2-monothiodiolato)(oxo)rhenium(V) (46)

From 100 mg $Tp'ReO_3$, 60.89 mg of triphenylphosphine, and 43.83 mg (0.561 mmol) 2-mercaptoethanol, 70 mg (0.12 mmol, 64.63%) greenish blue product was obtained. ^1H NMR (C_6D_6): δ 2.17 (s, 3H), 2.21 (s, 3H), 2.50 (s, 3H), 2.59 (s, 3H), 2.68 (s, 3H), 2.79 (s, 3H), 3.30 (ddd, 1H, J = 3.00, 5.70, 8.70 Hz), 3.63 (ddd, 1H, J = 5.40, 6.30, 8.70 Hz), 5.23 (ddd, 1H, J = 5.40, 6.00, 7.20 Hz), 5.51 (s, 1H), 6.03 (ddd, 1H, J = 3.00, 5.70, 7.80 Hz), 5.97 (s, 1H), 6.07 (s, 1H) ppm. ^{13}C NMR ($CDCl_3$): 12.74, 15.69, 17.16, 23.08, 27.91, 32.00, 64.38, 90.96, 107.88, 108.36, 108.63, 143.23, 145.77, 147.49, 153.94, 154.55, 157.91 ppm. IR (KBr pellet): 3121.60 (w), 2925.09 (m), 2851.74 (w), 2535.06 (w), 1545.34 (s), 1451.39 (s), 1416.16 (s), 1382.09 (m), 1379.01 (m), 1207.23 (s), 1069.47 (m), 1044.19 (w), 1020.24 (w), 955.14 (s), 939.70 (w), 862.30 (w), 816.31 (w), 782.02 (w), 692.43 (w) cm^{-1}. MS (FAB): 576.1 (M^+)

3.7 Synthesis and Characterization of Hydrido-*tris*-(3,5-dimethyl-1-pyrazolyl)borato (ethane-1-thio-2-methyl-1,2-diolate)(oxo)rhenium(V) (47)

From 100 mg Tp'ReO_3, 60.89 mg of triphenylphosphine, and 39.63 mg (0.43 mmol) 1-mercapto-propane-2-ol, the greenish blue crude product was obtained. The product was purified by chromatography on silica gel. Elution with 1:1 dichloromethane/hexane was used to elute the greenish blue products. The *syn* (53 mg, 0.09 mmol, 47.82%) and *anti* (40 mg, 0.067 mmol, 36.10%) isomers were isolated as separate bands. The stereochemistry of these two compounds was determined by the NOE experiment discussed in results and discussion chapter (Page 30-33.)

Spectroscopic data for *syn*-isomer:

^{1}H NMR ($CDCl_3$): δ 2.04 (d, 3H, J = 6.30 Hz), 2.16 (s, 3H), 2.22 (s, 3H), 2.48 (s, 3H), 2.59 (s, 3H), 2.70 (s, 3H), 2.77 (s, 3H), 3.37 (dd, 1H, J = 10.80, 12.01 Hz), 3.47 (dd, 1H, J = 6.30, 12.31 Hz), 4.80 (ddq, 1H, J = 10.80, 6.30, 6.30 Hz), 5.53 (s, 1H), 5.96 (s, 1H), 6.06 (s, 1H) ppm. ^{13}C NMR ($CDCl_3$): 13.36, 14.52, 16.28, 17.10, 23.06, 23.44, 32.00, 51.31, 98.64, 107.89, 108.47, 108.55, 143.26, 145.59, 147.59, 153.94, 154.81, 157.90 ppm. IR (KBr pellet): 3132.18 (w), 2961.78 (w), 2923.80 (w), 2834.06 (w), 2540.91 (w), 1544.91 (s), 1451.97 (s), 1416.78 (m),

1383.18 (m), 1371.04 (m), 1207.45 (s), 1067.59 (s), 1044.89 (w), 1007.16 (w), 954.14 (s), 917.23 (w), 862.20 (w), 816.81 (w), 782.85 (w), 693.98 (w), 654.97 (m) cm^{-1}. MS (FAB): 590.1 (M^+)

Spectroscopic data for *anti*-isomer:

^1H NMR ($CDCl_3$): δ 1.47 (d, 3H), 2.16 (s, 3H), 2.28 (s, 3H), 2.49 (s, 3H), 2.57 (s, 3H), 2.68 (s, 3H), 2.79 (s, 3H), 2.87 (dd, 1H, J = 6.6, 11.7 Hz), 3.84 (dd, 1H, J = 6.6, 11.7 Hz), 5.51 (s, 1H), 5.82 (hex, 1H, J = 6.3 Hz), 5.97 (s, 1H), 6.04 (s, 1H) ppm. ^{13}C NMR ($CDCl_3$): 12.82, 14.12, 16.28, 16.98, 23.06, 25.42, 32.00, 55.75, 93.96, 107.95, 108.43, 108.51, 143.10, 145.91, 147.02, 153.67, 154.63, 157.64 ppm. IR (KBr pellet): 3129.76 (w), 2958.29 (m), 2924.18 (m), 2514.12 (w), 1545.50 (s), 1451.53 (s), 1417.05 (s), 1382.47 (s), 1370.50 (s), 1208.04 (s), 1187.37 (m), 1067.53 (s), 1045.77 (m), 1011.75 (w), 985.51 (w), 953.76 (s), 925.88 (m), 877.97 (w), 862.00 (m), 841.31 (m), 817.06 (m), 782.47 (m), 692.58 (m), 664.75 (w), 645.03 (m) cm^{-1}. MS (FAB): 590.1 (M^+)

3.8 Synthesis and Characterization of Hydrido-*tris*-(3,5-dimethyl-1-pyrazolyl)borato (phenylethanedithiodiolato)(oxo)rhenium(V) (45)

From 100 mg $Tp'ReO_3$, 60.89 mg of triphenylphosphine, and 128.06 mg (0.752 mmol) phenylethanedithiol, the dark brown crude product was obtained. The crude product was purified by chromatography on silica gel; elution with 1:1

dichloromethane/hexane was used to elute the dark brown product, which is a mixture of *syn* and *anti* isomers (120 mg, 0.18 mmol, 47.81%). The following is the spectroscopic data for a 1:1 mixture of *syn* and *anti* isomers of phenylethanedithiodiolate complex: ^{1}H NMR (C_6D_6): δ 1.97 (s, 6H), 2.21 (s, 3H), 2.23 (s, 3H), 2.25 (s, 3H), 2.26 (s, 3H), 2.49 (s, 3H), 2.62 (s, 3H), 2.95 (s, 3H), 3.11 (s, 3H), 3.15 (s, 3H), 3.18 (s, 3H), 3.88 (dd, 1H, J = 7.82, 12.21 Hz), 4.30 (t, 1H, J = 12.48 Hz), 4.56 (dd, 1H, J = 6.31, 12.62 Hz), 4.62 (dd, 1H, J = 6.89, 12.21 Hz), 4.83 (dd, 1H, J = 6.31, 12.62 Hz), 5.30 (s, 1H), 5.31 (s, 1H), 5.36 (t, 1H, J = 7.28 Hz), 5.57 (s, 1H), 5.62 (s, 1H), 5.67 (s, 2H), 7.0-7.9 ppm (m, 10H). The assignment of each signal by using COSY, HSQC, and NOE experiments was discussed in results and discussion chapter (Page 38-47). ^{13}C NMR (C_6D_6): 12.49, 12.50, 12.50, 12.51, 12.54, 12.56, 16.16, 16.18, 16.21, 16.25, 17.23, 17.82, 52.43, 59.79, 66.00, 77.93, 107.98, 108.02, 108.77, 108.79, 108.82, 108.87, 127.19, 128.74, 128.81, 128.83, 128.95, 142.54, 142.61, 144.27, 145.09, 145.24, 145.44, 145.69, 146.53, 154.06, 154.27, 155.70, 155.96, 156.09, 156.38 ppm. IR (KBr pellet): 3024.52 (w), 2924.03 (w), 2546.94 (w), 2363.89 (w), 2344.96 (w), 1719.77 (w), 1545.21 (s), 1490.51 (w), 1450.53 (s), 1414.36 (s), 1382.59 (m), 1365.90 (m), 1284.64 (w), 1210.38 (s), 1065.79 (m), 1039.80 (m), 984.88 (w), 942.03 (s), 861.17 (w), 817.26 (w), 694.42 (m), 646.77 (w) cm^{-1}. MS (FAB): 668.3 $(M+H)^{+}$

3.9 Synthesis and Characterization of Styrene Trithiocarbonate (48)

Styrene oxide (0.5 ml, 4.38 mmol), potassium hydroxide (0.55 g, 9.86 mmol), and carbon disulfide (0.66 ml, 10.95 mmol) were allowed to stir in 30 ml of methanol for 24 h at room temperature. The methanol was removed in vacuo by using rotary evaporator. The crude product was then extracted with 50 mL of 3:1 toluene/water mixture. The organic layer was washed with 10 mL of diluted hydrochloric acid, 10 mL of saturated solution of sodium bicarbonate, and 20 mL of water respectively. The organic layer was dried over sodium sulfate. Evaporation of organic layer gave 0.86 g yellow needles (4.05 mmol, 92.63%) ^{1}H NMR ($CDCl_3$): δ 4.04 (dd, 1H, J = 5.77, 12.08 Hz), 4.18 (dd, 1H, 10.43, 12.07 Hz), 5.65 (dd, 1H, 5.62, 10.29 Hz), 7.45 (m, 5H) ppm. ^{13}C NMR ($CDCl_3$): 50.14, 64.61, 127.91, 129.62, 129.68, 135.60 ppm. IR (KBr pellet): 3027.54 (w), 1752.90 (w), 1582.12 (w), 1486.53 (w), 1450.31 (w), 1419.31 (w), 1284.73 (w), 1229.80 (w), 1220.44 (w), 1053.39 (s), 972.79 (w), 908.79 (w), 881.37 (s), 839.73 (w), 767.65 (m), 726.09 (m), 695.51 (m), 587.75 (w) cm^{-1}. MS (FAB): 213 $(M+H)^{+}$

3.10 Synthesis and Characterization of Phenylethanedithiol (49)

This reaction was performed under an argon atmosphere. To 5 mL of THF in a 3-neck flask, 1 M lithium aluminium hydride in diethylether (2.87 mL, 2.87 mmol) was added. The yellow solid styrene trithiocarbonate (200 mg, 2.87 mmol) was then sequentially added. The color of the solution changed from yellow to very pale yellow. The reaction was allowed to proceed for 1 h. Excess lithium aluminium hydride was eliminated by gradually adding wet THF, and then water. The reaction was filtered and dried over magnesium sulfate. Evaporation of solvent yielded a colorless liquid product (140 mg, 0.82 mmol, 87.5%). ^{1}H NMR ($CDCl_3$): δ 1.48 (dd, 1H, J = 7.54, 9.47 Hz), 2.29 (d, 1H, J = 5.63 Hz), 2.94 (ddd, 1H, J = 6.86, 9.33, 13.58 Hz), 3.10 (ddd, 1H, J = 7.69, 13.73, 15.37 Hz), 4.10 (ddd, 1H, J = 5.76, 6.86, 7.68 Hz), 7.30 (m, 5H) ppm. ^{13}C NMR ($CDCl_3$): 34.84, 47.74, 127.92, 128.43, 129.46, 142.28 ppm. IR (neat): 3060.12 (w), 3027.31 (w), 2918.71 (w), 2849.70 (w), 2553.48 (w), 1600.64 (w), 1490.45 (s), 1452.23 (s), 1422.71 (w), 1382.60 (w), 1160.29 (w), 1075.82 (w), 760.55 (w), 697.64 (s) cm^{-1}. MS (CI): 170 (M^+)

3.11 Reaction of Rhenium Dioxo Complex and Ethylenesulfide

This reaction was done both with and without acid catalysis. For the acid-catalyzed conditions, the reaction was done under exactly the same condition as the synthesis of Tp' rhenium dithiodiolate complex. Tp'ReO_3 (100 mg, 0.188 mmol), triphenylphosphine (60.89 mg, 0.236 mmol), ethylene sulfide (22.61 mg, 0.376

mmol), *p*-toluenesulfonic acid (2.0 mg, 0.012 mmol), ground molecular sieves (0.5 g) were allowed to stir at room temperature for 15 h in 25 mL of THF. The dark yellow solution was filtered, and the solvent was removed in vacuo. The product was purified by chromatography on silica gel. Elution with 1:1 dichloromethane/hexane was used to elute the dark brown products. Surprisingly, the major product from this reaction was Tp' rhenium(oxo)ethanedithiodiolate (33.70 mg, 30.30 %). The ^{1}H NMR spectrum of this product was identical to the Tp' rhenium dithiodiolate that was made independently from ethanedithiol and Tp' rhenium trioxo complex. ^{1}H NMR ($CDCl_3$): δ 2.12 (s, 3H), 2.16 (S, 3H), 2.52 (s, 6H), 2.89 (s, 6H), 3.58 (AA'BB', 2H), 4.09 (AA'BB', 2H), 5.49 (s, 1H), 6.03 (S, 2H) ppm. The splitting pattern of AA'BB' system in this compound is identical to the one from Tp' rhenium dithiodiolate, and Rf of this compound is exactly the same as Tp' rhenium dithiodiolate.

For the reaction without acid catalyst, the procedure was the same as an acid-catalyzed reaction, which was shown above, but in this case, none of *p*-toluenesulfonic acid was added. After filtration, the solvent was removed by rotary evaporation, and a dark brown crude product was obtained. The product was purified by means of column chromatography with 1:1 dichloromethane/hexane as an eluent. The major product, which is a dark brown solid, was characterized by ^{1}H NMR. The spectrum was identical to Tp' rhenium ethanedithiodiolate complex (29.64 mg, 26.65%).

3.12 Reaction of Rhenium Dioxo Complex and Cyclohexene Sulfide

This reaction was also done under both acid-catalyzed and non acid-catalyzed conditions. For the acid-catalyzed conditions, the procedure for synthesis of Tp' rhenium ethanedithiodiolate complex was used. Tp'ReO_3 (100 mg, 0.188 mmol), triphenylphosphine (60.89 mg, 0.236 mmol), cyclohexene sulfide (42.94 mg, 0.377 mmol), *p*-toluenesulfonic acid (2.0 mg, 0.012 mmol), ground molecular sieves (0.5 g) were allowed to stir at room temperature for 15 h in 25 mL of THF. The green solution was filtered, and the solvent was removed in vacuo. The dark green crude product was purified by chromatography on silica gel. Elution with 1:1 dichloromethane/hexane was used to elute the green products. Several attempts were made in order to isolate the green products, which appeared to be 3 different compounds in TLC chromatography. However, only the mixture of first and second compounds can be isolated.

For the reaction without acid catalyst, the procedure was the same as an acid-catalyzed reaction, which was shown above, but no acid was added. The isolation was done under the same procedure, and the product was exactly the same from TLC. Namely, only a mixture of first and second green compounds was isolated. ^1H NMR and ^{13}C NMR of this fraction was identical to the one from acid-catalyzed reaction. The spectroscopic data for this product is shown as follow: ^1H NMR ($CDCl_3$): δ 0.86 (s, 2H), 0.88 (s, 3H), 0.91 (s, 1H), 1.30 (broad s, 1H), 2.30 (broad s, 2H), 2.17 (s, 6H), 2.23 (s, 1H), 2.34 (s, 5H), 2.47 (s, 3H), 2.56 (s, 3H),

2.27 (s, 3H), 2.83 (s, 3H), 2.89 (s, 2H), 2.92 (1H), 3.32 (broad s, 1H), 3.77 (broad s, 1H), 5.54 (s, 1H), 5.77 (broad s, 1H), 5.89 (s, 1H), 5.97 (s, 1H), 6.01 (s, 1H) ppm. ^{13}C NMR ($CDCl_3$): 12.64, 12.73, 12.76, 12.85, 13.02, 13.09, 14.16, 14.31, 14.40, 14.45, 14.53, 14.68, 16.92, 17.24, 20.37, 22.95, 24.15, 25.85, 26.54, 27.45, 29.59, 64.72, 66.30, 66.60, 68.86, 107.94, 108.37, 108.39, 108.66, 108.73, 129.23, 130.53, 131.13, 153.19 ppm. IR (KBr pellet): 2546.55 (w), 2364.94 (w), 2345.61 (w), 1544.73 (s), 1450.14 (s), 1415.03 (m), 1383.41 (m), 1370.21 (m), 1209.03 (s), 1069.42 (s), 983.61 (w), 958.30 (w), 908.29 (s), 864.25 (w), 814.73 (w), 783.93 (w), 692.52 (w), 646.33 (w), 623.00 (w) cm^{-1}. MS (FAB): 678.2 (M^+)

3.13 Procedure for Recrystallization of Hydrido-*tris*-(3,5-dimethyl-1-pyrazolyl)borato(ethane-1,2-dithiodiolato)(oxo)rhenium(V) (44)

Crystals of hydrido-*tris*-(3,5-dimethyl-1-pyrazolyl)borato(ethane-1,2-dithiodiolato) (oxo)rhenium(V) were grown by recrystallization from CH_3CN/H_2O. The saturated solution of the ethanedithiodiolate complex was prepared by adding the dark brown solid to acetonitrile in a 5 mL vial until no more solid dissolved. The vial was sealed and left overnight. Then the solution and remaining solid were filtered, and the filtrate was placed into the new 5 mL vial tube. This solution was then placed into a saturated atmosphere of water vapor at 10 °C. The crystals of ethanedithiodiolate were collected by filtration after 5 days.

3.14 Single-Crystal X-ray Diffraction Analysis of Hydrido-*tris*-(3,5-dimethyl-1-pyrazolyl)borato(ethane-1,2-dithiodiolato)(oxo)rhenium(V) (44)

The following details of crystallographic analysis were provided by Dr. Alexandre Yokochi. Determination of the crystallographic parameters, data collection and structure solution and refinement was done according to the literature[58]. Specific details are shown as follow: A small block of approximate dimensions 0.1 x 0.1 x 0.1 mm^3 was mounted on the end of a Pyrex fiber using some epoxy glue. An automated routine was used to find and center 15 reflections with $15° < 2\theta < 35°$. The crystal was indexed and the lattice parameters refined against this list. The reflection list was then expanded to include 65 reflections with $35° < 2\theta < 57.3°$. All unique data, including a small set of redundant reflections were collected (-1 – h, -1 – k, -1 – l). Given the high linear absorption coefficient of this compound for Cu Kα radiation, the data were corrected for the effects of absorption anisotropy by means of a face indexed method, as programmed in the program Platon[59].

Examination of the systematic extinctions, coupled with the fact that the intensity statistics calculated for this data set strongly suggested an acentric space group[60], led to the choice of the space group $P2_12_12_1$ (#19). The structure was solved by direct methods as programmed in SHELXS-90[61]. This solution clearly showed the ReN_3OS_2 core of the molecule. The solution was expanded by successive cycles of least squares refinements followed by Fourier synthesis using the program SHELXL-97[62]. In the final cycle of least squares refinement all non-

hydrogen atoms were refined using anisotropic thermal displacement coefficients. All hydrogen atoms were placed in idealized positions, and their displacement parameters were fixed to be either 1.5 times (methyl group hydrogen atoms) or 1.2 times (all other hydrogen atoms) that of the atom to which it was attached. Refinement of the Flack parameter yielded a value of -0.001(19), indicating that the model depicted corresponds the correct absolute structure[63]. The chirality of the compound arises from the torsion of the *tris*-pyrazolylborate ligand about the imaginary Re-B axis.

3.15 Cycloreversion Reaction of Hydrido-*tris*-(3,5-dimethyl-1-pyrazolyl) borato(oxo)(dithiodiolate) and (Monothiodiolate)rhenium(V) Complexes

The following method is a general procedure for the attempted cycloreversion reaction of Tp' rhenium dithiodiolates and monothiodiolates. To the dry sealable NMR tube, 5 mg of compound was added. A tiny crystal of 1,4-di-*tert*-butylbenzene was added as an internal standard. The NMR tube was place onto a double-manifold Schlenk line. The NMR tube was evacuated for 10 minutes. Deuterated benzene was vaccum transferred to the NMR tube until the level of solvent was about 4 cm. The NMR tube was then sealed and shaken until all of the solid dissolved. ^{1}H NMR of this solution was collected as soon as a clear solution was obtained. The mixture was then placed into a thermostated bath at 80° C for 2 hours, and the ^{1}H NMR was collected. The mixture was taken back to the thermostated bath and left overnight. A ^{1}H NMR spectrum was collected on the

next day. However, there was no significant change in the ^{1}H NMR spectrum. This observation led to the conclusion that the cycloreversion reaction did not proceed under these conditions. The same mixture was then place into the thermostat bath at 100° C for 2 hours, then overnight. ^{1}NMR spectra were collected after each period, and no significant change was observed. The temperature of the bath was increased to 120° C, and the same experiment was repeated. At this time, the mixture was left at 120° C for 7 days. Again, no significant change was observed from ^{1}H NMR spectrum. Integration of the dithiodiolate versus 1,4-di-*tert*-butylbenzene had changed by less than 3%.

The same procedure was used for all of the sulfur analogs of Tp' rhenium diolates synthesized in this study. However, from ^{1}H NMR spectrum, none of these compounds undergoes the cycloreversion reaction at the temperature up to 120° Celsius. This observation revealed the thermal stability of all of Tp' rhenium dithiodiolate and monothiodiolate complexes.

Chapter 4. Conclusions

Tp' rhenium dithiodiolate and monothiodiolate complexes were successfully synthesized. All the compounds were completely characterized. X-ray crystallographic analysis was performed for Tp' rhenium ethanedithiodiolate. Crystallographic data reveals an unusually flat dithiodiolate ring with a dihedral angle (C-S-S-C) of 12°. The solution conformation analyzed by using the Karplus relationship between coupling constants and dihedral angles shows a staggered geometry with a dihedral angle (C-S-S-C) of 38°. All of these complexes fail to cyclorevert at 120 °C for 7 days due to the thermodynamic stability of each compound. DFT calculations of cycloaddition of ethylene to tetrathioperrhenate anion also indicates the stability of rhenium dithiodiolate species. Reaction of Tp' rhenium dioxide species and ethylene sulfide both with and without acid catalysis gives an unexpected product, which is the Tp' rhenium ethanedithiodiolate complex. The mechanism for this process was proposed to initially form a coordinated episulfide intermediate, followed by selective reduction of Tp'ReO_2S complex by triphenylphosphine. However, the same reaction with cyclohexene sulfide gives a different product that cannot be completely characterized due to the separation problems.

Bibliography

1. R. Jira, W. Blau, and D. Grimm, *Hydrocarbon Proc.* **1976**, 97-100.

2. Ittel, S.D.; Parshall, G.W. *Homogeneous Catalysis*, 2nd Ed.; John Wiley & Sons: New York, 1992, 138.

3. Evans, D.A.; Bender, S.L.; Morris, J. *J. Am. Chem. Soc.* **1998**, 110, 2506.

4. Hanson, R.M.; Sharpless, K.B. *J. Org. Chem.* **1986**, 51, 1922.

5. Ittel, S.D.; Parshall, G.W. *Homogeneous Catalysis*, 2nd Ed.; John Wiley & Sons: New York, 1992, 149.

6. Trost, M.K.; Bergman, R.G. *Organometallics* **1991**, 10, 1172-8.

7. Mimoun, H.; Mignard, M.; Brechot, P.; Saussine, L. *J. Am. Chem. Soc.* **1986**, 108, 3711-8.

8. Carey, F.A. and Sundberg R.J. *Advanced Organic Chemistry*, 3rd Ed., Part B; Plenum: New York, 1990, 627.

9. Hanson, R.M.; Sharpless, K.B. *J. Org. Chem.* **1986**, 51, 1922.

10. Rossiter, B.E.; Katsiku, T.; Sharpless, K.B. *J. Am. Chem. Soc* **1981**, 103, 464.

11. Bianchini, C.; Meli, A. *Acc. Chem. Res.* **1998**, 31, 109-116.

12. Shaver, A.; El-khateeb, M.; Lebuis, A. M. *Angew. Chem., Int. Ed. Engl.* **1996**, 35, 2362.

13. Stiefel, E.I.; Matsumoto, K. *Transition Metal Sulfur Chemistry: Biological and Industrial Significnce, ACS Symposium Series*, 653, American Chemical Society, Washington, DC, 1996, 154.

14. Riaz, U.; Curnow, O.; Curtis, M.D. *J. Am. Chem. Soc.* **1991**, 113, 1416.

15. Carey, F.A. and Sundberg R.J. *Advanced Organic Chemistry*, 3rd Ed., Part B; Plenum: New York, 1990, 624.

16. Rheenen, V.V.; Kelly, R.C.; Cha, D.Y. *Tetrahedron Lett.* **1976**, 1973.

17. Nugent, W.A.; Mayer, J.M. *Metal-Ligand Multiple Bonds*, John Wiley & Sons: New York, 1988, 252.

18. Criegee, R. *Justus Liebigs Ann. Chem.* **1936**, 522, 75-96.

19. Corey, E.J.; Noe, M.C.; Sharsan, S. *J. Am. Chem. Soc.* **1993**, 115, 3828-3829.

20. Sharpless, K.B. *J. Am. Chem. Soc.* **1977**, 3120.

21. Jorgensen, K.A.; Hoffmann, R. *J. Am. Chem. Soc.* **1986**, 108, 1867-1876.

22. Carey, F.A. and Sundberg R.J. *Advanced Organic Chemistry*, 3rd Ed., Part A; Plenum: New York, 1990, 193

23. Gable, K.P.; Phan, T.N. *J. Am. Chem. Soc.* **1993**, 115, 3036-3037.

24. Gable, K.P.; Phan, T.N. *J. Am. Chem. Soc.* **1994**, 116, 833-839.

25. Gable, K.P.; Juliette J.J.J. *J. Am. Chem. Soc.* **1995**, 117, 955-962.

26. Gable, K.P.; Juliette J.J.J. *J. Am. Chem. Soc.* **1996**, 118, 2625-2633.

27. Gable, K.P.; AbuBaker, A.; Zientara, K.; Wainwright, A.M. *Organometallics* **1999**, 18, 173-179.

28. Murray, H.H.; Wei, L.W.; Sherman, S.E.; Greaney, M.A.; Eriksen, K.A.; Carstensen, B.; Halbert, T.R.; Stiefel, E.I. *Inorg. Chem.* **1995**, 34, 841-853.

29. Goodman, J.T.; Rauchfuss, T.B. *J. Am. Chem. Soc.* **1999**, 121, 5017-5022.

30. Dopke, J.A.; Wilson, S.R.; Rauchfuss, T.B. *Inorg. Chem.* **2000**, 39, 5014-5021.

31. Rappe', A.K.; Goddard, W.A. *J. Am. Chem. Soc.* **1982**, 104, 3287-3294.

32. Coucouvanis, D. *Adv. Inorg. Chem.* **1998**, 45, 1-73.

33. Tisato, F.; Bolzati, C.; Duatti, A.; Bandoli, G.; Refsco, F. *Inorg. Chem.* **1993**, 32, 2042-2048.

34. Lente, G.; Shan, X.; Guzei, I.A.; Espenson, J.H. *Inorg. Chem.* **2000**, 39, 3572-3576.

35. Gable, K.P.; Brown, E.C. *Organometallics* **2000**, 19, 944-946.

36. Dubois, M.R.; Kanney, J.; Noll, B.C. *Organometallics* **2000**, 19, 4925-4928.

37. Chianelli, R.R.; Pecoraro, T.A.; Halbert, T.R.; Pan, W.H.; Stiefel, E.I. *J. Catal.* **1984**, 86, 226-230.

38. Gable, K.P.; AbuBaker, A.; Zientara, K.; Wainwright, A.M. *Organometallics* **1999**, 18, 173-179

39. Gunther, H. *NMR Spectroscopy*, 2nd Ed.; John Wiley & Sons, 1995, 181-187.

40. Culvenor, C. C. J.; Davies, W.; Pausacker, K. H. *J. Chem. Soc.* **1946**, 1050-2.

41. Iqbal, S. M.; Owen, L.N. *J. Chem. Soc.*, **1960**, 1030-6.Gable, K.P.; AbuBaker, A.; Zientara, K.; Wainwright, A.M. *Organometallics* **1999**, 18, 173-179.

42. Atkins, P.W. *Physical Chemistry*, 5th Ed.; Oxford University Press, 1995, 637.

43. Pachler, K.G.R. *J. Chem. Soc., Perkin Trans.2* **1972**, 1936-1940.

44. http://www.spectroscopynow.com/Spy/tools/proton-proton.html

45. Gable, K.P.; AbuBaker, A.; Zientara, K.; Wainwright, A.M. *Organometallics* **1999**, 18, 173-179

46. Goodman, J.T.; Rauchfuss, T.B. *J. Am. Chem. Soc.* **1999**, 121, 5017-5022.

47. Dopke, J.A.; Wilson, S.R.; Rauchfuss, T.B. *Inorg. Chem.* **2000**, 39, 5014-5021.

48. Rappe', A.K.; Goddard, W.A. *J. Am. Chem. Soc.* **1982**, 104, 3287-3294.

49. Coucouvanis, D. *Adv. Inorg. Chem.* **1998**, 45, 1-73.

50. Gable, K.P.; Chuawong, P.; Yokochi, A.F.T. *Organometallics*, submitted.

51.Gable, K.P.; Brown, E.C. *Organometallics* **2000**, 19, 944-946.

52. Shriver, D.F.; Drezdzon, M.A. *Manipulation of Air-sensitive Compounds* Wiley: New York, 1986.

53. Nuts: NMR Utility Transform Software for Windows 95/NT. 1D Version, Acorn NMR Inc., 1997.

54. Trofimenko, S. *J. Am. Chem. Soc.* **1967**, 89, 3170-3177.

55. Herrmann, W. A., et al, *Inorg. Chem.* , **1992**, 31, 4431-32.

56. Mayer, J.M., Matano, Y.; Northcutt, T.O.; Brugman, J.; Bennett, B.K.; Lovell, S. *Organometallics.* , **2000**, 19, 2781-2790.

57. Gable, K.P.; AbuBaker, A.; Zientara, K.; Wainwright, A.M. *Organometallics* **1999**, 18, 173-179.

58. Blakemore, P. R., Kim, S.-K., Schulze, V. K., White, J. D., Yokochi, A. F. T. *J. Chem. Soc. Perkin Trans. 1*, In Press.

59. PLATON/PLUTON - (a) Spek, A. L. *Acta Crystallogr.*, **1990**, *A46*, C34. (b) PLATON, A Multipurpose Crystallographic Tool, Utrecht University, Utrecht, The Netherlands, Spek, A. L. 1998.

60. See, for example, Schwarzenbach, D.; Abrahams, S. C.; Flack, H. D.; Gonschorek, W.; Hahn, T.; Huml, K.; Marsh, R. E.; Prince, E.; Robertson, B. E.; Rollet, J. S.; Wilson, A. J. C. *Acta Crystallogr.* **1989**, *A45*, 63-75.

61. Sheldrick, G. M. *Acta Crystallogr.* **1990**, *A46*, 467.

62. Sheldrick, G. M. In *Crystallographic Computing 6*; Flack, H. D., Parkanyi, L., Simon, K., Eds.; Oxford University Press: Oxford, 1993.

63. Flack, H. D. *Acta Crystallogr.* **1983**, *A39*, 876.

64. Dobler, C.; Mehltretter, G.; Beller, M. *Angew. Chem. Int. Ed.* **1999**, 38, 3026-3028.

65. Thomas, J.A.; Davison, A. *Inorg. Chim. Acta* **1991**, 190, 231-235

APPENDIX

Appendix. Crystallographic Data

Table A.1: Crystal Data and Structure Refinement for Tp'Re(O)(SCH_2CH_2S)

Identification code	KG120100	
Empirical formula	$C_{17}H_{26}BN_6OReS_2$	
Formula weight	591.57	
Temperature	290(2) K	
Wavelength	1.54178 Å	
Crystal system	Orthorhombic	
Space group	$P2_12_12_1$ (#19)	
Unit cell dimensions	a = 8.5673(5) Å	α= 90°.
	b = 11.4116(12) Å	β= 90°.
	c = 22.8696(19) Å	γ = 90°.
Volume	2235.9(3) $Å^3$	
Z	4	
Density (calculated)	1.757 Mg/m^3	
Absorption coefficient	12.535 mm^{-1}	
F(000)	1160	
Crystal size	0.10 x 0.10 x 0.10 mm^3	
Theta range for data collection	3.87 to 67.41°.	
Index ranges	-10<=h<=1, -1<=k<=13, -27<=l<=1	
Reflections collected	2817	
Independent reflections	2627 [R(int) = 0.0332]	
Completeness to theta = 67.41°	92.9 %	
Absorption correction	Analytical	
Max. and min. transmission	0.3670 and 0.3670	
Refinement method	Full-matrix least-squares on F^2	
Data / restraints / parameters	2627 / 0 / 255	
Goodness-of-fit on F^2	1.069	
Final R indices [I>2sigma(I)]	R1 = 0.0284, wR2 = 0.0721	
R indices (all data)	R1 = 0.0300, wR2 = 0.0744	
Absolute structure parameter	0.000(19)	
Extinction coefficient	0.00035(4)	
Largest diff. peak and hole	0.868 and -0.831 $e.Å^{-3}$	

Table A.2: Atomic Coordinates (x 10^4) and Equivalent Isotropic Displacement Parameters ($Å^2$x 10^3) for Tp'Re(O)(SCH_2CH_2S)

U(eq) is defined as one third of the trace of the orthogonalized U^{ij} tensor.

	x	y	z	U(eq)
Re	7505(1)	6943(1)	1685(1)	24(1)
O	9412(5)	7090(4)	1812(2)	36(1)
B	6748(12)	4706(7)	803(3)	37(2)
N(11)	7856(6)	5058(4)	1801(2)	30(1)
N(12)	7595(10)	4276(4)	1356(2)	38(1)
C(11)	8701(10)	4490(6)	2206(3)	40(2)
C(12)	9277(13)	5032(8)	2762(4)	60(3)
C(13)	8998(12)	3353(7)	2022(4)	53(2)
C(14)	8264(13)	3254(6)	1487(4)	53(2)
C(15)	8100(20)	2183(7)	1102(5)	104(6)
N(21)	5216(6)	6230(5)	1328(2)	31(1)
N(22)	5219(7)	5251(6)	979(3)	36(1)
C(21)	3693(8)	6564(7)	1387(3)	39(2)
C(22)	3171(10)	7588(8)	1729(5)	63(3)
C(23)	2743(8)	5778(7)	1081(4)	50(2)
C(24)	3710(11)	4985(7)	834(3)	48(2)
C(25)	3310(14)	3937(9)	471(5)	83(3)
N(31)	8073(7)	6681(5)	759(2)	33(1)
N(32)	7778(7)	5610(5)	494(2)	35(2)
C(31)	9024(8)	7292(7)	408(3)	38(2)
C(32)	9657(12)	8472(9)	548(4)	61(3)
C(33)	9329(11)	6617(8)	-89(3)	53(2)
C(34)	8517(10)	5594(7)	-29(3)	46(2)
C(35)	8439(16)	4558(9)	-429(4)	75(3)
S(1)	6708(2)	8827(1)	1524(1)	41(1)
S(2)	6427(2)	7115(2)	2591(1)	42(1)
C(41)	6148(16)	9443(8)	2221(5)	78(3)
C(42)	6192(16)	8677(9)	2730(4)	71(3)

Table A.3: Bond Lengths [Å] and Angles [°] for Tp'Re(O)(SCH_2CH_2S)

Re-O	1.668(5)
Re-N(11)	2.189(5)
Re-N(31)	2.193(5)
Re-N(21)	2.275(5)
Re-S(2)	2.2757(18)
Re-S(1)	2.2858(17)
B-N(22)	1.505(11)
B-N(32)	1.531(11)
B-N(12)	1.539(10)
N(11)-C(11)	1.342(9)
N(11)-N(12)	1.371(7)
N(12)-C(14)	1.334(9)
C(11)-C(13)	1.387(11)
C(11)-C(12)	1.499(11)
C(13)-C(14)	1.380(12)
C(14)-C(15)	1.513(12)
N(21)-C(21)	1.366(9)
N(21)-N(22)	1.374(8)
N(22)-C(24)	1.369(10)
C(21)-C(23)	1.398(10)
C(21)-C(22)	1.477(11)
C(23)-C(24)	1.351(12)
C(24)-C(25)	1.495(11)
N(31)-C(31)	1.340(9)
N(31)-N(32)	1.388(8)
N(32)-C(34)	1.353(9)
C(31)-C(33)	1.397(12)
C(31)-C(32)	1.487(12)
C(33)-C(34)	1.366(12)
C(34)-C(35)	1.497(12)
S(1)-C(41)	1.808(10)

S(2)-C(42)	1.822(10)
C(41)-C(42)	1.455(14)
O-Re-N(11)	86.7(2)
O-Re-N(31)	88.0(2)
N(11)-Re-N(31)	87.2(2)
O-Re-N(21)	160.6(2)
N(11)-Re-N(21)	79.0(2)
N(31)-Re-N(21)	78.2(2)
O-Re-S(2)	103.30(18)
N(11)-Re-S(2)	91.76(15)
N(31)-Re-S(2)	168.60(17)
N(21)-Re-S(2)	90.42(15)
O-Re-S(1)	103.10(18)
N(11)-Re-S(1)	170.13(15)
N(31)-Re-S(1)	92.21(17)
N(21)-Re-S(1)	91.19(16)
S(2)-Re-S(1)	86.82(7)
N(22)-B-N(32)	110.3(6)
N(22)-B-N(12)	108.8(6)
N(32)-B-N(12)	108.8(7)
C(11)-N(11)-N(12)	106.6(6)
C(11)-N(11)-Re	129.2(5)
N(12)-N(11)-Re	121.9(4)
C(14)-N(12)-N(11)	109.4(6)
C(14)-N(12)-B	131.8(6)
N(11)-N(12)-B	118.6(5)
N(11)-C(11)-C(13)	110.0(7)
N(11)-C(11)-C(12)	124.4(7)
C(13)-C(11)-C(12)	125.6(8)
C(14)-C(13)-C(11)	105.1(7)
N(12)-C(14)-C(13)	108.9(7)
N(12)-C(14)-C(15)	122.3(8)
C(13)-C(14)-C(15)	128.7(8)
C(21)-N(21)-N(22)	106.6(6)

C(21)-N(21)-Re	133.5(5)
N(22)-N(21)-Re	119.9(4)
C(24)-N(22)-N(21)	108.6(6)
C(24)-N(22)-B	131.7(6)
N(21)-N(22)-B	119.6(6)
N(21)-C(21)-C(23)	109.2(7)
N(21)-C(21)-C(22)	124.2(7)
C(23)-C(21)-C(22)	126.6(7)
C(24)-C(23)-C(21)	106.3(6)
C(23)-C(24)-N(22)	109.3(6)
C(23)-C(24)-C(25)	128.9(9)
N(22)-C(24)-C(25)	121.9(9)
C(31)-N(31)-N(32)	107.8(6)
C(31)-N(31)-Re	130.0(5)
N(32)-N(31)-Re	120.1(4)
C(34)-N(32)-N(31)	108.3(6)
C(34)-N(32)-B	131.9(6)
N(31)-N(32)-B	119.8(5)
N(31)-C(31)-C(33)	108.4(7)
N(31)-C(31)-C(32)	124.3(7)
C(33)-C(31)-C(32)	127.3(8)
C(34)-C(33)-C(31)	107.1(7)
N(32)-C(34)-C(33)	108.4(7)
N(32)-C(34)-C(35)	122.0(8)
C(33)-C(34)-C(35)	129.5(8)
C(41)-S(1)-Re	107.6(4)
C(42)-S(2)-Re	106.7(3)
C(42)-C(41)-S(1)	117.7(6)
C(41)-C(42)-S(2)	116.8(6)

Table A.4: Anisotropic Displacement Parameters ($Å^2 x\ 10^3$) for $Tp'Re(O)(SCH_2CH_2S)$

The anisotropic displacement factor exponent takes the form:
$-2\pi^2[\ h^2\ a^{*2}U^{11} + ...\ + 2\ h\ k\ a^*\ b^*\ U^{12}\ ]$

	U^{11}	U^{22}	U^{33}	U^{23}	U^{13}	U^{12}
Re	23(1)	25(1)	24(1)	-1(1)	-1(1)	-2(1)
O	28(2)	39(3)	41(3)	0(2)	2(2)	2(2)
B	55(5)	31(3)	26(4)	-7(3)	-6(4)	10(4)
N(11)	39(4)	26(2)	24(3)	-2(2)	-4(2)	2(2)
N(12)	55(3)	28(2)	30(3)	0(2)	-11(4)	0(4)
C(11)	44(4)	37(4)	39(4)	14(3)	-5(4)	3(4)
C(12)	87(7)	42(4)	51(5)	9(4)	-37(5)	-8(5)
C(13)	83(6)	33(4)	44(5)	7(4)	-6(5)	22(4)
C(14)	91(6)	34(3)	34(4)	3(3)	-8(5)	18(5)
C(15)	211(18)	35(4)	67(7)	-5(4)	-37(9)	37(8)
N(21)	23(2)	37(3)	32(3)	-9(3)	-4(2)	-1(2)
N(22)	43(3)	35(3)	29(3)	-5(3)	-5(3)	-7(3)
C(21)	24(3)	49(4)	44(4)	0(4)	2(3)	-4(3)
C(22)	28(3)	63(5)	99(8)	-21(5)	1(5)	11(4)
C(23)	30(4)	60(4)	59(5)	5(4)	-14(3)	-14(4)
C(24)	54(5)	50(5)	40(5)	-5(4)	-13(4)	-25(4)
C(25)	87(8)	66(6)	95(8)	-27(6)	-29(7)	-18(7)
N(31)	39(3)	40(3)	21(3)	3(3)	3(2)	-3(3)
N(32)	47(4)	32(2)	25(3)	3(2)	3(3)	5(3)
C(31)	37(4)	50(4)	28(4)	12(4)	12(3)	-5(4)
C(32)	71(6)	62(5)	50(5)	15(5)	10(5)	-18(5)
C(33)	56(5)	72(5)	30(4)	11(5)	18(4)	4(5)
C(34)	59(5)	51(4)	27(4)	0(4)	10(4)	14(4)
C(35)	118(9)	68(6)	40(5)	-16(5)	23(6)	22(7)
S(1)	42(1)	26(1)	55(1)	-1(1)	-8(1)	4(1)

S(2)	45(1)	48(1)	32(1)	-9(1)	10(1)	-6(1)
C(41)	99(9)	44(5)	92(8)	-38(5)	17(7)	18(6)
C(42)	106(9)	65(6)	43(5)	-19(5)	9(6)	2(7)

Table A.5: Hydrogen Coordinates (x 10^4) and Isotropic Displacement Parameters ($Å^2$x 10^3) for Tp'Re(O)(SCH_2CH_2S)

	x	y	z	U(eq)
H(0)	6555	4042	541	45
H(12A)	10144	5538	2678	90
H(12B)	9604	4426	3026	90
H(12C)	8453	5479	2938	90
H(13)	9568	2781	2218	64
H(15A)	7148	2236	883	156
H(15B)	8077	1492	1342	156
H(15C)	8969	2142	838	156
H(22A)	3261	7418	2139	95
H(22B)	2103	7760	1636	95
H(22C)	3811	8253	1635	95
H(23)	1660	5798	1053	60
H(25A)	4022	3882	148	124
H(25B)	2263	4013	326	124
H(25C)	3389	3242	706	124
H(32A)	9026	9061	364	92
H(32B)	10710	8531	407	92
H(32C)	9645	8587	964	92
H(33)	9965	6826	-402	63
H(35A)	9101	4690	-762	113
H(35B)	7383	4448	-559	113

H(35C)	8783	3870	-225	113
H(41A)	6824	10107	2299	94
H(41B)	5094	9744	2184	94
H(42A)	5232	8788	2948	85
H(42B)	7044	8930	2979	85